International Immunology, Vol. 17, No. 5, pp. 549–558
doi:10.1093/intimm/dxh237

Presence and distribution of neural crest-derived cells in the murine developing thymus and their potential for differentiation

Hidetoshi Yamazaki[1,2], Emi Sakata[2], Toshiyuki Yamane[2,3], Ayano Yanagisawa[2], Kuniya Abe[4], Ken-Ichi Yamamura[5], Shin-Ichi Hayashi[2] and **Takahiro Kunisada[2,6]**

[1]Division of Regenerative Medicine and Therapeutics, Department of Genetic Medicine and Regenerative Therapeutics, Institute of Regenerative Medicine and Biofunction, Tottori University Graduate School of Medical Science, Yonago 683-8503, Japan
[2]Division of Immunology, Department of Molecular and Cellular Biology, School of Life Science, Faculty of Medicine, Tottori University, Yonago 683-8503, Japan
[3]Department of Pathology, Stanford University School of Medicine, Stanford, CA 94305, USA
[4]Technology and Development Team for Mammalian Cellular Dynamics, RIKEN Tsukuba Institute, BioResource Center, Tsukuba 305-0074, Japan
[5]Division of Developmental Genetics, Institute of Molecular Embryology and Genetics, Kumamoto University, Kumamoto 862-0976, Japan
[6]Department of Tissue and Organ Development, Regeneration and Advanced Medical Science, Gifu University Graduate School of Medicine, Gifu 500-8705, Japan

Keywords: colony assay, *Cre*, melanocytes, organogenesis, protein 0

Abstract

Neural crest (NC) cells are multipotent cells that can differentiate into melanocytes, neurons, glias and myofibroblasts. They migrate into the fetal thymus on embryonic day (E) 12 in mice and may participate in thymic organogenesis. Although the abnormality of migration and distribution of NC cells in the thymus results in immunodeficiency, the spatial and temporal presence of their progeny cells has not been defined in detail. In this study, we traced NC-derived cells based on the myelin protein zero gene promoter-*Cre*-mediated excision. We demonstrated that large numbers of NC-derived cells in the thymus were detected on E11.5 to E16.5 but rarely on E17.5. A colony formation assay of single thymic cells demonstrated that multipotent cells with the potential to differentiate into melanocytes, neurons and/or glias were present in the E14.5 and E15.5 but not in the E17.5 fetal thymus. Furthermore, we confirmed that these multipotent cells were NC-derived cells. Taken together, these findings imply that multipotent NC-derived cells are present in the developing thymus, but rarely in this organ at a later stage, suggesting that NC-derived cells may play roles in thymic organogenesis at an early embryonic stage.

Introduction

Neural crest (NC) cells migrate and differentiate into a variety of cell lineages such as melanocytes, neurons, glial cells, myofibroblasts, chondrocytes and osteoblasts (1–5). NC cells migrating in the pharyngeal arch are thought to participate in the organogenesis of the craniofacial area, thyroid gland, heart and thymus (6–10). The failure or aberrant migration and abnormal distribution of NC cells result in a condition known as DiGeorge syndrome. It is characterized by defective aortic arch patterning, a conotruncal heart, thymic and parathyroid aplasia/hypoplasia including immunodeficiencies and craniofacial anomalies (11, 12). These reports suggest that NC-derived cells may contribute to thymic organogenesis. Using avian systems, Le Douarin and her colleagues proposed the participation of avian NC cells in thymic organogenesis (4, 8). Using *Wnt1-Cre* reporter mice, Jiang *et al.* reported that murine cardiac NC-derived cells were detected around the thymus (13). However, in the murine thymus, the distribution or potential for differentiation of NC-derived cells has been rarely substantiated.

The thymus is composed of three major cell lineages, i.e. hematopoietic cells (including T lymphocytes), epithelial cells

Correspondence to: H. Yamazaki; E-mail: yamazaki@grape.med.tottori-u.ac.jp
Received 29 November 2004, *accepted* 7 February 2005
Transmitting editor: T. Kurosaki
Advance Access publication 18 April 2005

that support T lymphocyte differentiation and mesenchymal cells surrounding the thymus (6, 14, 15). Experiments using chick and quail inter-species chimeras indicate that NC-derived cells differentiate into inter-lobular and outer thymic mesenchymal cells but not into hematopoietic cells or thymic epithelial cells (7, 8). Furthermore, ablation of NC cells by the microcautery of neural folds induces thymic abnormalities that reduce the numbers of both mesenchymal and epithelial cells (16, 17).

In this study, we employed the expression of the myelin protein zero (*P0*) gene, an indicator of NC-derived cells (18–21), and we chased NC-derived cells and assessed their presence, distribution, expression of adhesion molecules and potential in the murine thymus. It has been thought that melanocyte precursors might be distinct from neuronal and glial cell precursors or lose the potential to differentiate into neuron or glial cell lineages before or soon after the initiation of NC cell migration (22–27). Therefore, the demonstration of NC-derived cells that maintain the potential to differentiate into not only melanocytes but also neurons and glial cells would indicate the presence of NC-derived cells including multipotent NC cells. To examine the potential of NC-derived cells in the thymus, we developed a colony formation assay using single thymic cells incubated in the presence of endothelin 3 (ET3). ET3 is known to promote the survival and differentiation of not only melanocytes but also glial cells in avian cultures (28–30). Using these two types of analyses, we showed that at least double- or triple-potent NC-derived cells exist during early thymogenesis, and observed a severe reduction in their number at the late embryonic stages of thymus development in mice.

Methods

Mice

Mice carrying *Cre* recombinase driven by the protein 0 (*P0*) promoter were produced as described (19), and *Rosa26R* mice were obtained from Kumamoto University (18). C57BL/6 mice were purchased from Japan Clea (Tokyo, Japan).

Determination of genotypes of transgenic mice

Genomic DNA was prepared, and transgenes were detected by use of PCR. The respective sense and anti-sense primers used for PCR were as follow—*LacZ*: 5′-GGT AGC AGA GCG GGT AAA CT-3′/5′-ATC TGA CGG GCT CCA GGA GT-3′ and *Cre*: 5′-GGA CAT GTT CAG GGA TCG CCA GGC G-3′/5′-GCA TAA CCA GTG AAA CAG CAT TGC TG-3′. PCR was performed by incubation at 94°C for 4 min, followed by 35 cycles of incubation at 93°C for 1 min, 58°C for 1 min and 72°C for 1 min and a final extension at 72°C for 7 min.

Histological analysis

For detection of LacZ activity, whole embryos and tissues were fixed in PBS solution (pH 7.4) containing 2% formaldehyde (Wako), 0.2% glutaraldehyde (Wako) and 0.02% NP-40 (Sigma). After washing, samples were stained with a solution containing Bluo-Gal (GIBCO-BRL) in *N,N′*-dimethylformamide (Wako) until the desired color intensity had been obtained. For preparation of tissue sections, thymi were embedded in a polyester wax (BDH Laboratory Supplies). Sections were prepared at a 7-μm thickness, and stained with hematoxylin and eosin.

Fluorescein di-β-D-galactopyranoside loading and flow cytometric analysis

Single-cell suspensions from thymi of embryonic day (E) 12.5 to 3.5-day-old mice were prepared by digestion with collagenase D (Roche), Dispase II (Roche) and trypsin/EDTA (GIBCO-BRL). Fluorescein di-β-D-galactopyranoside (FDG) staining was carried out essentially as described (31). To reduce background fluorescence, we incubated the cells in FDG staining medium [4% fetal bovine serum (FBS; JRH)/10 nM HEPES (pH 7.3)/PBS] containing 1 mM chloroquine for 30 min at 37°C, 5% CO_2. Cells were then loaded with FDG (Molecular Probe, Eugene, OR, USA) by osmotic shock. Briefly, after the cells had been allowed to equilibrate in a water bath at 37°C for 10 min, an equal volume of pre-warmed 2 mM FDG in sterile water was rapidly mixed with the cell suspension. After exactly 2 min of incubation at 37°C, the FDG loading was stopped; and cells were suspended in ice-cold staining medium containing 10 μg ml^{-1} propidium iodide for 5 min at 4°C. Then, cells were blocked with rabbit serum, and stained with biotin-conjugated rat anti-mouse mAbs against CD45 (30-F11; BD PharMingen) and integrins α4 (P/S-2; a gift from K. Miyake, Tokyo University), α5 (5H10-27; BD PharMingen), αV (RMV-7; BD PharMingen), β1 (KMI-6; a gift from K. Miyake, Tokyo University) and β3 (2C9.G2; BD PharMingen). The stained cells were further incubated with *R*-PE-labeled streptavidin (Southern Biotech Associate, Inc.). The stained cells were analyzed by using an EPICS-XL flow cytometer (Coulter).

Induction of melanocytes from thymic cells

Single-cell suspensions from thymi of E12.5 to 3.5-day-old mice were prepared as described above. The prepared cells were inoculated into 24-well plates (Corning Costar) with ST2 stromal cells (32), and cultured in α-MEM (GIBCO-BRL) containing 10% FBS (Hyclone), supplemented with the following reagents: 10^{-7} M dexamethasone (DEX, Sigma), 40 nM human recombinant ET3 (Peptide Institute) and 1 nM BQ788, an antagonist of endothelin receptor B (ETR-B; Phoenix Pharmaceuticals, Inc.). Cultures were fed every third day by replacing the medium with 2 ml of fresh medium. After 3 weeks, the cells were harvested by treatment with 0.25% trypsin/EDTA, and the number of melanocytes was counted.

Induction of melanocytes, neurons and glias in thymic clonal cell cultures

Thymic cell suspensions from E14.5, E15.5 and E17.5 embryos were prepared as described above. Then, 1–2 × 10^5 cells were inoculated into six-well plates (Corning Costar) with ST2 stromal cells (32), and cultured in α-MEM supplemented with 10% FBS, 10^{-7} M DEX, 40 nM human ET3, 1 nM heregulin (Phoenix Pharmaceuticals, Inc.) and 1 nM forskolin (Phoenix Pharmaceuticals, Inc.) for the simultaneous induction of melanocytes, neurons and glia. Cultures were fed every third day by replacing the medium with 2 ml of fresh medium. After the cells had been cultured for 14 days, they were stained

with LacZ to confirm the presence of NC-derived cells and with specific antibodies to identify the types of colonies. For detection of LacZ activity, the cells were fixed in PBS solution (pH 7.4) containing 0.25% glutaraldehyde. After having been washed, they were stained with a solution containing Bluo-Gal (GIBCO-BRL) in *N,N'*-dimethylformamide for 8 h.

Antibodies and immunohistochemistry

On serial days after induction of the differentiation of thymic cells, the cultured cells were stained separately with the polyclonal rabbit anti-mouse dopachrome tautomerase (Dct) antibody (provided by V. Hearing; Laboratory of Cell Biology, National Institutes of Health, Bethesda, MD, USA; 33) or with the following mAbs: rat anti-mouse nerve growth factor receptor p75 (p75) (AB-N02; ATSBIO, Inc.), mouse anti-mouse β-tubulin III (TUJI; Babco), mouse anti-porcine glial fibrillary acidic protein (GFAP) (GA-5; Neomarker, Inc.), rat anti-mouse erythroid lineage cells (TER119; PharMingen) or mouse anti-human HLA-DQ (Neomarker, Inc.). The cultured cells were fixed with 2% PFA. After a washing, the endogenous peroxidase activity was blocked with 0.3% hydrogen peroxide, and the cells were then incubated with the first antibody. The bound antibody was visualized by subsequent incubation with biotin-conjugated goat antibodies against mouse, rat or rabbit IgG followed by streptavidin–HRP (HistoMark™ Streptavidin–HRP Kit). After having been washed, the cells bearing immunocomplexes were visualized by using a Diaminobenzidine Reagent Set (Kirkegaard and Perry Laboratories, Inc.).

Statistical analysis

Data were presented as mean ± SD. Statistical significance was assessed by using Student's *t*-test.

Results

Tracing NC-derived cells in the fetal thymus by using the P0-Cre/Rosa26R mouse system

To assess the presence of NC-derived cells in the thymus, we constructed mice carrying the *Cre* gene under the control of the *P0* promoter (*P0-Cre*), which expresses the *Cre* gene in the NC cell lineage (19). Crossing *P0-Cre* mice and *Rosa26R* mice, which carry *LoxP-LacZ* sequences, enabled us to trace NC-derived cells that had expressed the *P0* gene as LacZ-expressing cells. $LacZ^+$ cells were detected in organs including the mandible and heart, in which NC-derived cells were previously reported to be present, and in the thymus of E14.5 *P0-Cre/Rosa26R* double-transgenic (*Tg*) embryos (Fig. 1B). However, no $LacZ^+$ cells were detected in age-matched *Rosa26R* embryos that did not carry *P0-Cre Tg* (Fig. 1A).

Temporal differences in the presence of NC-derived cells in the thymus

To clarify the spatial and temporal presence of NC-derived cells in the developing thymus, we stained *P0-Cre/Rosa26R* mice or *Rosa26R* mice from E11.5 to E18.5 for LacZ. As shown in Fig. 2, large numbers of $LacZ^+$ (NC-derived) cells were detected in E11.5, E12.5, E14.5, E15.5 and E16.5 thymi, but these cells were rarely detected in the thymus beyond E17.5 in

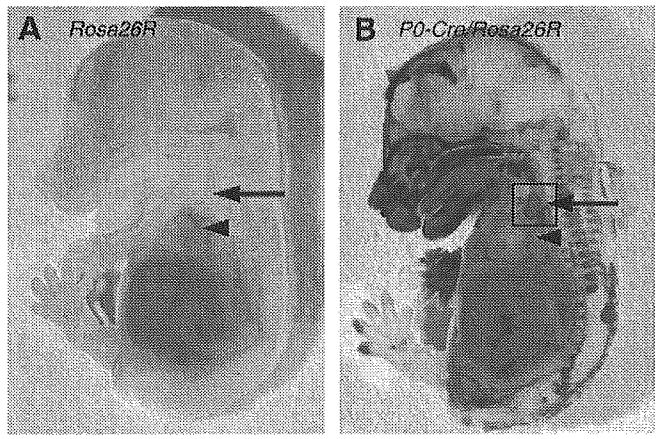

Fig. 1. Presence of NC-derived cells in the fetal thymus. Cells that expressed the *P0* gene were detected by staining of E14.5 *P0-Cre/Rosa26R* double-*Tg* mice for LacZ (B). $LacZ^+$ cells were present in the thymus (arrow) as well as in the face and heart (arrow head). No $LacZ^+$ cells were present in any tissues of age-matched *Rosa26R-Tg* mice (A).

P0-Cre/Rosa26R embryos. As NC-derived cells were still detected in the heart and craniofacial region of E18.5 *P0-Cre/Rosa26R* embryos, the present duration of NC-derived cells in the thymus might be distinct from that in other organs (Fig. 2B).

To confirm the results obtained by LacZ staining, we performed flow cytometric analysis using FDG, which allows $LacZ^+$ cells to be detected as living cells. Approximately 15% of the total thymic cells on E14.5, but only 2% on E18.5, were $LacZ^+$ cells (Fig. 3A). These results agree with the data on whole-mount embryos stained for LacZ and suggest that the number of NC-derived cells decreased in the developing thymus as it became older. Furthermore, we could rarely detect NC-derived cells in the post-natal thymus (data not shown).

Spatial distribution of NC-derived cells in the thymus

To assess the distribution of NC-derived cells in the thymus, we prepared E14.5 and E18.5 thymic sections and stained them with hematoxylin and eosin and for LacZ. In E14.5 sections, the fetal thymus was surrounded by $LacZ^+$ NC-derived cells (Fig. 3B). The region containing $LacZ^+$ cells corresponded to that of mesenchymal cells surrounding the thymus. However, only a few NC-derived cells were present in the E18.5 thymus, and their location was restricted to marginal sites close to the heart (Fig. 2B').

One-third (32%) of E13.5 total thymic cells were NC-derived ones (Fig. 3C, left graph). To assess the distribution of NC-derived cells at the marginal sites of the thymus, we treated E13.5 thymi with Dispase II to divide them into the mesenchymal and epithelial regions. It is known that digestion with Dispase II keep the basement membrane intact. Single-cell suspensions were then prepared from each region, and flow cytometric analysis was performed on them. When we used cells from the mesenchymal region surrounding the thymus, nearly half of the cells expressed LacZ. In contrast, the proportion of NC-derived cells was decreased in the population from the epithelial region (Fig. 3C). These results suggest

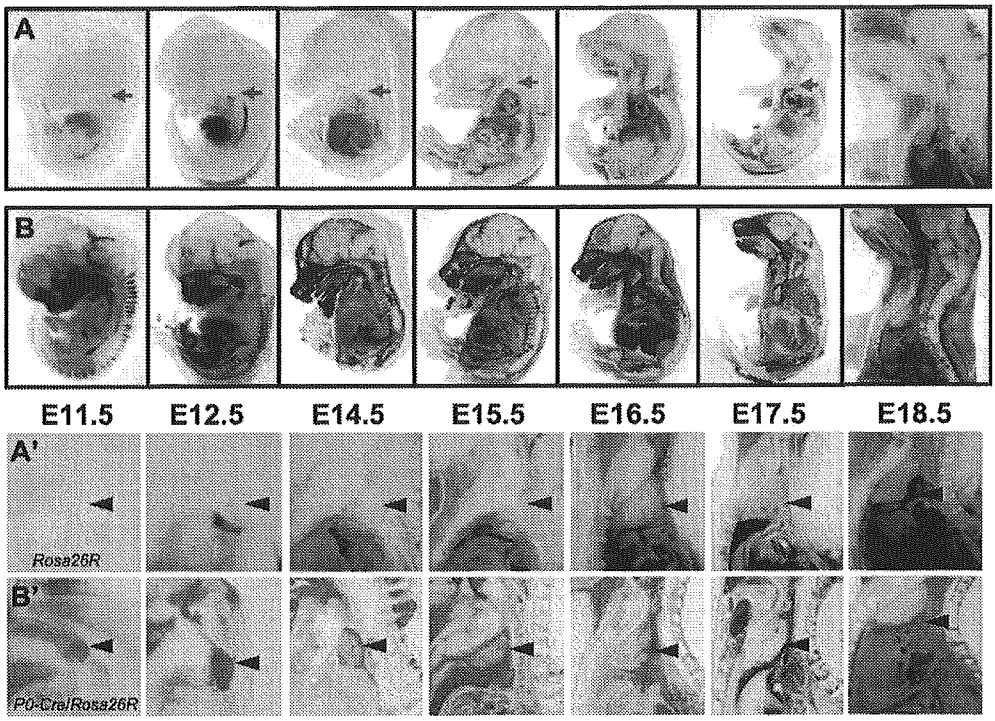

Fig. 2. Presence of NC-derived cells in the fetal thymus from E11.5 to E18.5. The thymi of E11.5 to E18.5 *Rosa26R-Tg* [A, A'(magnified)] and *P0-Cre/Rosa26R* double-Tg [B, B'(magnified)] mice were stained for LacZ (red arrows). Large numbers of LacZ$^+$ NC-derived cells were detected in the *P0-Cre/Rosa26R* double-*Tg* thymus; however, their number was reduced beyond E17.5. The arrows in (A) and (B) and the arrowheads in (A') and (B') point to the thymus.

that a majority of the NC-derived cells were distributed in the mesenchyme surrounding the thymus, although a few of them had invaded the thymic epithelium.

Characterization of NC-derived cells in the fetal thymus

To characterize NC-derived cells in the thymus, we examined the expression of adhesion molecules on NC-derived cells of *P0-Cre/Rosa26R* mice using flow cytometric analysis. First, we examined the expression of CD45 on E13.5 mesenchymal cells surrounding thymi. LacZ$^+$ cells rarely express CD45, indicating that NC do not contribute to hematopoietic cells in the thymus (data not shown). A majority of LacZ$^+$ cells in the E13.5 mesenchymal cells surrounding thymi express integrin α5, αV, β1 and β3, and half of the LacZ$^+$ cells express integrin α4 (Fig. 3D). However, larger numbers of LacZ-negative cells also express these molecules on the cell surface (Fig. 3D). It is known that mesenchymal cells are derived from both NC cells and mesodermal cells. These results may suggest that it is difficult to distinguish NC-derived mesenchymal cells from mesoderm-derived mesenchymal cells by the expression of adhesion molecules such as integrin family.

Presence of cells with the potential to differentiate into the melanocyte lineage in the fetal thymus

It is thought that melanocyte precursors might be distinct from neuronal and glial cell precursors or lose their potential to differentiate toward neuron or glial cell lineages before or soon after the initiation of NC cell migration (24, 26). In fact, mature pigmented melanocytes are not normally present in the thymus. If NC-derived cells in the thymus give rise to melanocytes, they may be multipotent cells before committing to the melanocyte lineage. Therefore, to assess the potential of NC-derived cells in the murine thymus, we first investigated whether these cells could differentiate into melanocytes. Cells from C57BL/6 wild-type fetal and neonatal thymi were cultured on ST2 stromal cells with ET3 and DEX for 3 weeks (34). Pigmented melanocytes could be induced from E12.5, E14.5 and E15.5, but not from E18.5 or 3.5-day-old thymi (Table 1, Fig. 4A). In cultures of E14.5 thymic cells, the number of melanocytes was significantly decreased in the presence of BQ788, an antagonist of ETR-B (Fig. 4A).

Subsequently, using thymic cells from *P0-Cre/Rosa26R* double-*Tg* mice or *Rosa26R* mice, we performed melanocyte induction by using the same experimental protocol. Large numbers of colonies in the cultures from *P0-Cre/Rosa26R* double-*Tg* mice consisted of LacZ$^+$ cells, and the majority of the cells with melanin granules expressed LacZ (Fig. 4C), whereas the *Rosa26R* cultures contained pigmented cells, but none was LacZ$^+$ (Fig. 4B). Therefore, almost all cells that differentiated into melanocytes had expressed the *P0-Cre* gene. The frequency of LacZ$^+$ cells forming colonies with pigmented melanocytes was ~1 per 10^4 thymic cells (Table 3). Thus, a small but significant number of NC-derived cells in the fetal thymus were able to differentiate into melanocytes. The period when LacZ$^+$ cells were present in the fetal thymus was

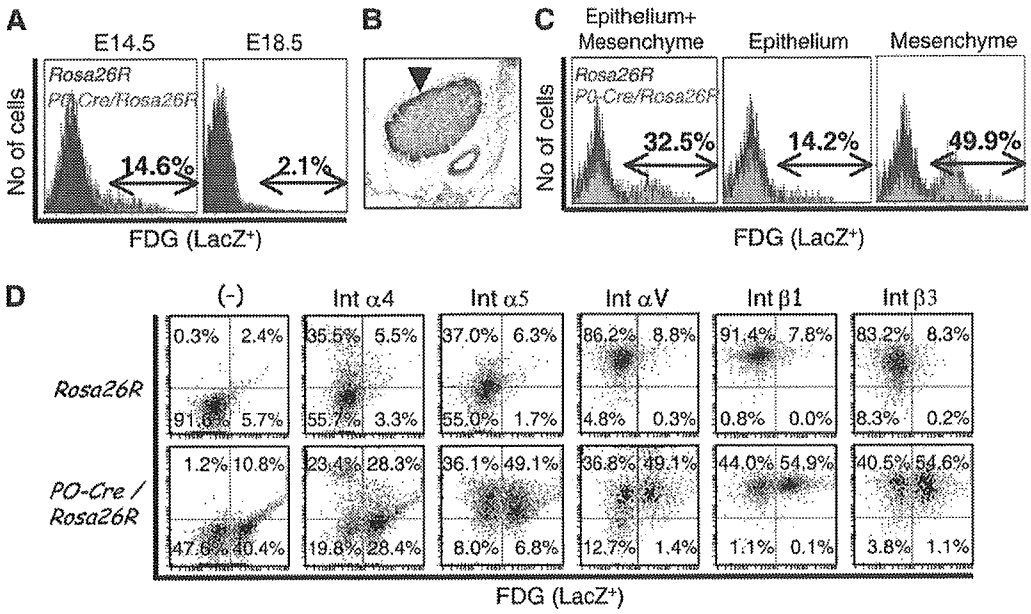

Fig. 3. Flow cytometric analysis of NC-derived cells in the thymus using FDG. (A) Cells from E14.5 or E18.5 thymi of *P0-Cre/Rosa26R* mice or *Rosa26R* mice were dissociated, and flow cytometric analysis was performed on the dissociated cells. Sections of E14.5 (B) and E18.5 (data not shown) thymi of *P0-Cre/Rosa26R* double-*Tg* mouse were stained for LacZ and also stained with hematoxylin and eosin. LacZ$^+$ cells were present in the area surrounding the thymus (B: arrowhead). No LacZ$^+$ cells were observed in the thymi of *Rosa26R* mice (data not shown). Next, E13.5 thymi were divided into mesenchyme and epithelium by treatment with Dispase II. (C) Cells from mesenchyme, epithelium and both were dissociated into single cells, and flow cytometric analysis was then performed on them. (D) The expression of adhesion molecules such as α4, α5, αV, β1 and β3 integrins on the mesenchymal cells surrounding thymi of E13.5 *P0-Cre/Rosa26R* mice. First, cells were stained with FDG to detect NC-derived cells, and then stained with antibodies against integrins.

mostly consistent with that when melanocyte precursors were present (Table 1). These results further confirm that LacZ$^+$ cells in the thymus of *P0-Cre/Rosa26R* mice are derived from NCs.

Next, to detect immature melanocyte lineage cells, we stained cultured cells with an antibody directed against Dct, which is specifically expressed on melanocyte precursors or 'melanoblasts' (33). Both Dct$^+$ melanoblasts and pigmented melanocytes were induced in the presence of ET3 and DEX (Fig. 4G), but neither of these types of cells was induced with DEX only (Fig. 4D and E). As neither Dct$^+$ cell (data not shown) nor pigmented melanocyte was detected in the E14.5 thymus, NC-derived cells prior to expressing the *Dct* gene might be stimulated by mainly ET3–ETR-B signaling to give rise to Dct$^+$ melanoblasts and pigmented melanocytes.

Table 1. Induction of melanocytes from fetal and post-natal C57BL/6 thymi in culture

	No. of melanocyte-containing cultures/No. of cultures examined				
Cells from +/+	E12.5 2/5[a]	E14.5 2/4[a]	E15.5 4/8	E18.5 0/6	D3.5 0/6

Two hundred thousand cells from fetal to 3.5-day-old (D3.5) thymi of C57BL/6 (+/+) mice were cultured with ST2 cells in the presence of ET3 and DEX. After 3 weeks, pigmented melanocytes were observed under a light microscope.
[a]Several thymic lobes were mixed and cultured in the case of E12.5 and E14.5 embryos to obtain 2 × 10^5 thymic cells, while only a pair of thymic lobes were cultured in the case of embryos from E15.5 or thereafter. Similar results were obtained in another independent experiment.

Presence of NC-derived cells in the fetal thymus with the potential to differentiate into multi-lineage cells

To determine whether NC-derived cells with the potential to differentiate into lineages other than the melanocyte lineage were present in the fetal thymus, we performed *in vitro* colony assays in the presence of ET3 with or without heregulin and forskolin, which strongly direct the differentiation of NC cells toward the glial cell lineage (35). Single cells from C57BL/6 thymi proliferated and formed a colony on day 14 of culture. The colonies from E14.5 or E15.5 thymic cells were characterized by the expression of p75 (a neuron and/or glial marker), β-tubulin III (a neuron-specific marker) or GFAP (a glia-specific marker) (Fig. 5). In some experiments, colonies were stained with a mixture of three antibodies against p75, β-tubulin III and GFAP (Fig. 5G and H). Colonies lacking both pigmented melanocytes and cells stained with antibodies directed against neurons and/or glias were omitted from the counting.

We identified three types of colonies: (i) pigmented melanocytes with melanin granules but no cells expressing neuronal or glial cell markers (named melanocyte colonies, Fig. 5A), (ii) p75$^+$ (Fig. 5B), β-tubulin III$^+$ or GFAP$^+$ cells (data not shown) but no melanocytes (neuron and/or glial colonies) and (iii) melanocytes and p75$^+$ (Fig. 5C), β-tubulin III$^+$ (Fig. 5D) or GFAP$^+$ cells (Fig. 5E) or cells stained by any three of the antibodies (Fig. 5H) (mixed colonies). As shown in Table 2, 4.5% (1 of 23 total colonies generated) of the colonies from

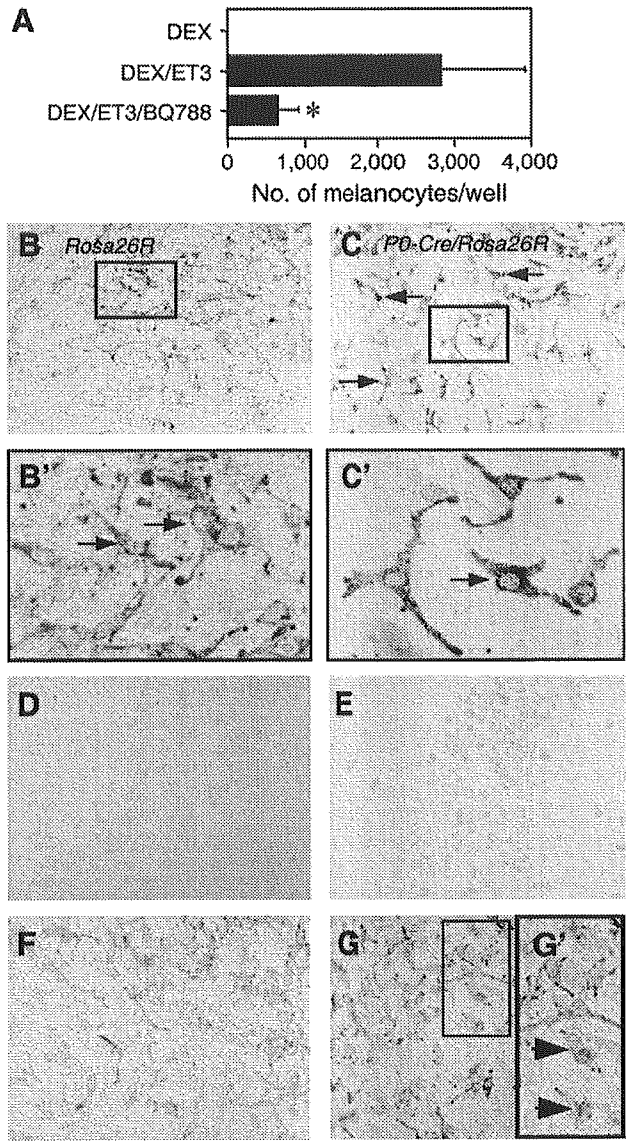

Fig. 4. Presence of cells with the potential to differentiate into melanocytes in the E14.5 thymus. (A) C57BL/6 E14.5 fetal thymic cells (2×10^5 per well) were cultured on ST2 stromal cells with DEX, DEX plus ET3 or DEX plus ET3 plus BQ788 for 3 weeks. The number of pigmented melanocytes (black cells) was then counted. Data are expressed as the mean ± SD of triplicate cultures. Asterisk indicates those significantly different from cultures with DEX + ET3 ($P < 0.05$). Next, E14.5 thymic cells from *P0-Cre/Rosa26R* double-*Tg* (C) and *Rosa26R-Tg* (B) mice were cultured in the presence of ET3. After 14 days, the cultured cells were stained for LacZ. The *P0-Cre/Rosa26R-Tg* cultures contained cells that were both pigmented (black) and $LacZ^+$ (blue) [C, C'(magnified); arrows], whereas the *Rosa26R* cultures contained pigmented cells, but none was $LacZ^+$ [B, B'(magnified); arrows]. Cultured cells treated with DEX (D, E) or with DEX + ET3 (F, G) were stained with rabbit anti-Dct antibody [E, G, G'(higher magnification)] to detect melanocyte precursors (melanoblasts: arrows) or with rabbit serum (D, F) as a control.

fetal thymi were $p75^+$ neuronal and/or glial colonies without melanocytes (Fig. 5B). Approximately 79% of the colonies from thymic cells (18/23) were melanocyte colonies, and 16% (4/23) were mixed colonies (Table 2). The formation of these mixed colonies of either melanocytes and neurons or melanocytes and glial cells thus indicate the presence of multipotent NC-derived cells (5, 36–38).

Using *P0-Cre/Rosa26R* double-*Tg* mice, we confirmed that the mixed colony-forming cells were NC-derived cells that expressed the *P0* gene (Fig. 5H). In a single colony (Fig. 5F), $LacZ^+$ cells with melanin granules (arrows in Fig. 5H) and cells stained by the mixture of antibodies directed against neurons and/or glias (arrowhead in Fig. 5H) co-existed. Pigmented melanocytes did not express p75, β-tubulin III or GFAP (Fig. 5C–E and H). These results indicate that multipotent NC-derived cells were present in the fetal thymus. In this culture, half of the colonies were melanocyte colonies, as was the case for cultures from wild-type mice, 15% of them were mixed colonies containing both p75/β-tubulin/$GFAP^+$ and pigmented cells and 30% of the colonies were neuronal and/or glial colonies containing p75/β-tubulin/$GFAP^+$ (Table 3).

NC-derived colony-forming cells were rarely detected in the E17.5 thymus

We showed that multipotent NC-derived cells were present in the E14.5 and E15.5 thymi (Fig. 5). When we assessed whether multipotent NC-derived cells were present in the thymus at late embryonic stages, few colonies were detected in cultures from the E17.5 thymus (Fig. 5I), confirming the rarity of NC-derived cells in the thymus after E17.5, as shown from the analysis of the *P0-Cre/Rosa26R* mice (Fig. 2).

Discussion

In this study, we showed that *P0-Cre/Rosa26R* mice were useful to trace NC-derived cells not only *in vivo* but also *in vitro*. Using these systems, we showed that NC-derived cells were mainly present in the area surrounding the thymus during E11.5 to E16.5 but were decreased in number beyond E17.5 and that NC-derived cells with the potential to differentiate into melanocyte, neuron and glia cell lineages were detected only during this same period.

Tracing NC-derived cells by using P0 promoter sequences

There is no specific marker for murine NC cells, unlike the case of HNK-1 for chickens and rats (39). Therefore, the promoters of *Pax3*, *Conexin43* and *Wnt1* genes have been used to detect the cranial NC cells containing cardiac NC cells (13, 40, 41). *Pax3-LacZ* and *Conexin43-LacZ* mice have provided the most reliable markers for the study of cardiac NC cell fate. Using mice bearing these markers, Waldo *et al.* detected NC cells in the E14 heart and thymus, but the expression of these transgenes was extinguished in mid- to late gestation (40). To trace the presence of NC-derived cells, we employed the promoter sequence of the *P0* gene, which promotes expression in migrating NC cells. The *P0* promoter sequence-driven *Cre* system as well as the human plasminogen activator–*Cre* system is useful for detecting not only cranial but also trunk NC-derived cells (19–21, 42), whereas the *Wnt1* promoter system allows the tracing of cranial NC cells only (13). We detected a large number of $LacZ^+$ cells in the E12.5 to E15.5 thymi of *P0-Cre/Rosa26R* mice, whereas the number was significantly decreased in E17.5 thymi and thereafter. Flow cytometric analysis confirmed the presence of $LacZ^+$ cells

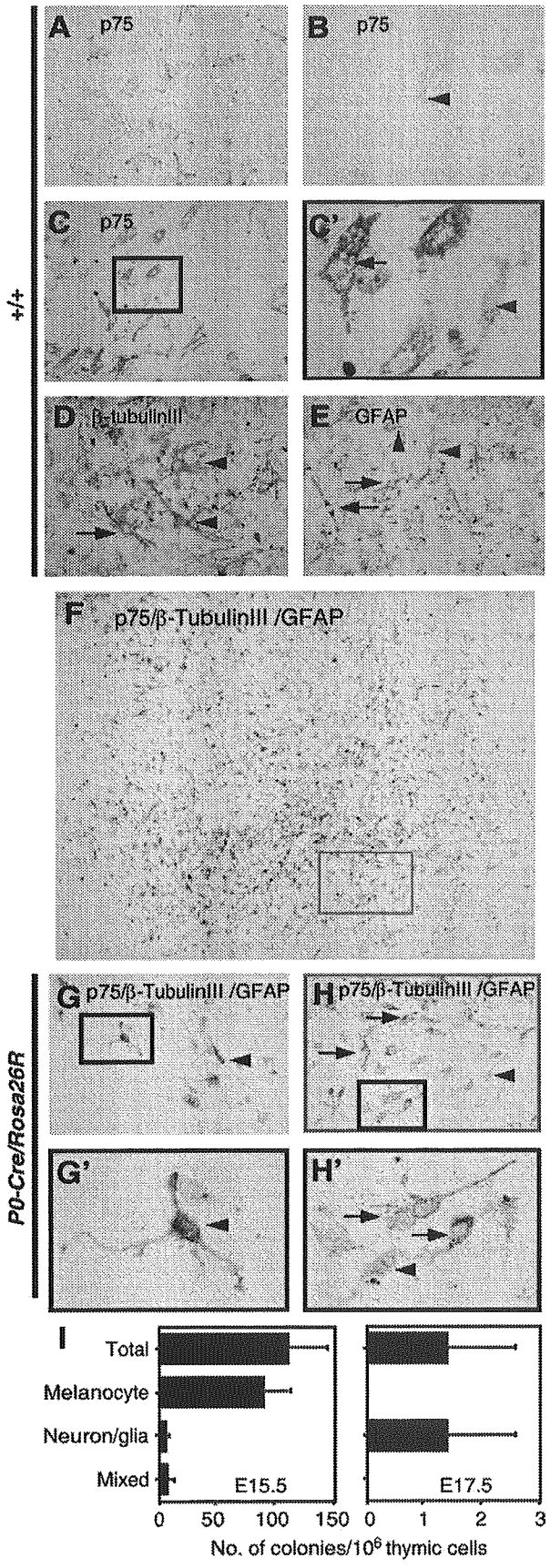

(~15%) in the E14.5 thymus and showed a significant reduction in their number (to ~2%) in the E18.5 thymus (Fig. 3). This finding is not unique to *P0-Cre/Rosa26R* mice, because similar observations were made when *Wnt1-Cre/Rosa26R* mice were examined (13). These results indicate that NC-derived cells contribute to thymic organogenesis and might explain why no melanocytes were induced in the E18.5 thymi of wild-type embryos (Table 1). However, a few NC-derived cells were still present in the E18.5 thymus; thus, it remains possible that they might have lost their potential to differentiate into melanocytes.

Presence of multipotent NC-derived cells in the fetal thymus

The melanocyte lineage has been thought to be derived only from the migrating NC cells through dorsolateral pathways (43). In contrast, posterior rhombencephalic NC cells that have migrated into posterior visceral arches have the potential to differentiate into neuronal cells, but not into melanocytes (3). Therefore, the commitment to the melanocyte lineage might occur in an early differentiation phase (3, 23, 24, 27). However, it is also reported that NC cells consist of heterogenous populations with the potential for differentiation (3, 4, 27). Therefore, there still remains the possibility that NC-derived cells in the developing thymus have a potential to differentiate only into melanocytes and neurons, or melanocytes and glial cells rather than multipotent NC-derived cells.

Recently, the presence of 'NC stem cells' that differentiate into glial cells, neurons and myofibroblasts in the sciatic nerve and gut of fetal rats was reported (5, 44). These stem cells were identified based on their expression of p75 molecules but not on that of other lineage markers for glial cells, neurons or myofibroblasts. However, these studies did not demonstrate the potential of these stem cells to differentiate into melanocytes. The culture conditions might not have permitted melanogenesis, or, alternatively, the stem cells isolated might have lacked melanogenic potential. In our culture system, we could not detect multipotent NC-derived cells with the potential to differentiate into myofibroblasts in the thymus. Our culture conditions might not have permitted such differentiation.

Fig. 5. Presence of multipotent NC-derived cells able to differentiate into melanocytes, neuronal and/or glial precursors in the fetal thymus. Colony formation by E15.5 (A–E) or E14.5 (F–H) fetal thymic cells was induced by culturing the cells on ST2 for 14 days in the presence of ET3, DEX, heregulin and forskolin. Colonies were stained with anti-p75 (A–C), anti-β-tubulin III (D), anti-GFAP (E) or a mixture of anti-p75, anti-β-tubulin III and anti-GFAP antibodies (F–H). Cells reactive with each antibody are stained brown (arrowheads), and black-pigmented cells (arrows) are melanocytes. (F) An NC-derived mixed colony with both melanocytes and neurons and/or glia cells. Colonies lacking both pigmented melanocytes and cells stained by antibodies directed against neurons and/or glia were omitted from the counting. NC-derived cells were detected as $LacZ^+$ cells that had expressed *P0-Cre Tg* by using *P0-Cre/Rosa26R-Tg* mice (F–H). Higher magnifications of the boxed regions in (G) and (H) are shown in (G') and (H'), respectively. Rat and mouse mAbs against irrelevant molecules were used as controls, and no positive cells were observed in the colonies (data not shown, see Methods). Two hundred thousand cells from E15.5 or E17.5 (I) fetal thymi from C57BL/6 (+/+) mice were cultured and stained as described. 'Mixed colonies' contained both melanocytes and $p75^+$ cells. This graph shows the number of colonies per 10^6 cells. Similar results were obtained in another independent experiment.

Table 2. Detection of melanocytes, neurons and/or glias in the colonies from fetal thymic cells

Colony type	No. of colonies/2 × 10^5 thymic cells
	+/+
Total colonies	22.7 ± 6.7 (100%)
Melanocyte colonies	18.0 ± 4.4 (79%)
Neuronal and/or glial colonies	1.0 ± 0.7 (4%)
Mixed colonies	3.7 ± 1.5 (16%)

Two hundred thousand cells from E15.5 fetal thymi from C57BL/6 (+/+) mice were cultured on ST2 in the presence of ET3, DEX, heregulin and forskolin. After 14 days, the cells were stained with anti-p75 mAb to identify the type of colonies (see caption of Fig. 5). A 'mixed colony' means that the colony contained both melanocytes and $p75^+$ cells. Similar results were obtained in another independent experiment.

Table 3. Detection of melanocytes, neurons and/or glias in the colonies from *P0-Cre/Rosa26R* E14.5 thymic cells

Colony type	No. of $LacZ^+$colonies/1 × 10^5 thymic cells
Total colonies	11.1 ± 5.3 (100%)
Melanocyte colonies	5.6 ± 2.7 (50%)
Neuronal and/or glial colonies	3.4 ± 1.4 (31%)
Mixed colonies	1.7 ± 1.9 (15%)
Others	0.4 ± 0.8 (4%)

One hundred thousand cells from E14.5 fetal thymi from *P0-Cre/Rosa26R* mice were cultured on ST2 in the presence of ET3, DEX, heregulin and forskolin. After 14 days, the cells were stained with a mixture of mAbs against p75/β-tubulin III/GFAP to identify the type of colonies (see caption of Fig. 5). A 'mixed colony' means that the colony contained both melanocytes and p75/β-tubulin III/$GFAP^+$ cells. The designation 'others' means $LacZ^+$ colonies melanocytes or p75/β-tubulin III/$GFAP^+$ cells. Similar results were obtained in another independent experiment.

Although large numbers of NC-derived cells were present in the thymus, they were rarely stained by specific antibodies directed against neurons, glias or melanocytes (data not shown). The majority of cells that expressed *P0* may have differentiated into cells of other lineages, or may have remained multipotent. The absence of melanocytes, neurons and glias in the normal thymus may result from the lack of proper microenvironmental factors for differentiation into these lineages. Here, we assessed only three cell lineages, namely melanocytes, neurons and glias. Analysis of additional cell lineages may reveal the precise roles of NC-derived cells in the thymus.

NC-derived cells and thymic organogenesis

The thymus is composed of both mesenchymal and epithelial cell components (6, 15). The thymic epithelium and mesenchyme are thought to be derived from the endoderm and/or ectoderm, and the mesoderm and/or NC cells, respectively (45–47). Thymic organogenesis is divided temporally into three stages, i.e. early (E9.5–E11), middle (E11.5–E15) and late (E15.5 to birth) (48). The early-stage-initiating thymic organogenesis is thought to be regulated by interactions between epithelial and mesenchymal cells (49–51).

In the middle stage, the patterning and initial epithelial differentiation occur in thymic rudiments, and T lymphocyte progenitors immigrate there (52–54). NC-derived cells are known to contribute to blood vessel formation, and they differentiate into pericytes surrounding vascular endothelial cells derived from the mesoderm (4, 55). Although in the middle stage, blood vessels have not yet formed in the thymus, mesenchymal cells surrounding the fetal thymus express the adhesion molecules that control migration and homing of hematopoietic cells. NC-derived cells are already present in the E11.5 thymus, meaning that cells of this lineage migrate into the thymus before hematopoietic cells. As shown in this study, NC-derived cells are mainly detected in the mesenchymal region surrounding the thymus, suggesting that NC-derived cells might help the immigration of T lymphocyte progenitors into the thymus (6, 8, 56).

Furthermore, we showed that integrin family members, such as integrin α4, α5, αV, β1 and β3 (Fig. 3), and CD44 (data not shown) were expressed on the cell surface of $LacZ^+$ cells (NC-derived cells) in the thymus. Previously, it was reported that signals via interaction between integrin receptors on mesenchyme and T progenitors are important for immigration of T progenitors into the thymus (57–59). These data suggest that NC-derived cells might play an important role in the immigration of T progenitor cells. Approximately 60% of the mesenchymal cells surrounding the E13.5 thymi express PDGFRα, and 70% in these $PDGFR\alpha^+$ cells are $LacZ^+$ cells (derived from NC-derived cells) (H.Y., unpublished data). $PDGFR\alpha^+$ cells are known to be important for thymic organogenesis because the mutation of this gene results in abnormalities of both the thymus and the heart (60, 61). As PDGFRα is expressed on both mesoderm-derived cells and NC-derived ones (62), it is not clear whether $PDGFR\alpha^+$ NC-derived cells are important for thymic organogenesis (62).

NC-derived cells and the late stages of thymic organogenesis

In the late stage, thymic epithelial cells have acquired the functional competence for supporting T lymphocyte development. In this stage, NC-derived cells are rarely detected, and T progenitors immigrate into the thymus through blood vessels in the cortical–medullar junction (63), suggesting that NC-derived cells might not be required during this stage. It is thought that these blood vessels are derived from the mesoderm and not from NC-derived cells. Petrie proposed that NC-derived cells have a minor role in thymic organogenesis after birth because few NC-derived cells were observed in the *Wnt1-Cre/Rosa26R* thymus at that time (13, 64).

Le Douarin and Jotereau (8) reported that avian NC cells contribute to thymic connective tissues, which are especially located in interlobular sites in the cortex and lining blood vessels in the cortex and medulla of the gland (65). Considering these previous reports, thymic NC-derived cells might likely be considered to be detected in the thymic cortex and medulla of murine embryos at a late stage. However, in E17.5 and E18.5 *P0-Cre/Rosa26R* mice as well as in *Wnt1-Cre/Rosa26R* mice, only a few NC-derived cells were present, and their location was restricted to the epithelial marginal sites of the thymic lobes (Figs 2 and 3). However, the possibility

cannot be ruled out that these promoters might not label NC cells completely. Alternatively, NC-derived cells that do not express *P0* or *Wnt1* might contribute to the thymic organogenesis at late embryonic stages. The roles of NC-derived cells may not be identical in avian and murine systems.

Conclusions

In this study, to assess both spatially and temporally the presence and the potential of NC-derived cells in the thymus, we traced NC-derived cells and developed a colony formation assay system. It is likely that NC-derived cells in the thymus retain multipotency, but are only present during a restricted period of thymogenesis.

In the heart and craniofacial area, NC-derived cells are continuously present and contribute to the organogenesis from the embryonic stage to adult life (13). However, the fact that NC-derived cells are only present in the thymus of early embryos may indicate the existence of an as yet unknown system that contributes to the organogenesis. Further studies using our system will yield important information on the role of NC-derived cells in thymic organogenesis.

Acknowledgements

We thank F. Melchers (Basel University and Max Planck Institute), M. Yoshino, M. Tsuneto and T. Yamada (Tottori University) for helpful discussions. We also gratefully acknowledge T. Shibahara (Tottori University) for maintenance of the mice and T. Shinohara for technical assistance. This work was supported by grants from Grants-in-Aid for Scientific Research from the Ministry of Education, Culture, Sports, Science, and Technology and from Research on Demential and Fracture, Health and Labour Sciences Research Grants, the Japanese Government, and by funding from the Molecular Medical Science Institute, Otsuka Pharmaceutical Co., Ltd.

Abbreviations

Dct	dopachrome tautomerase
DEX	dexamethasone
E	embryonic day
ET3	endothelin 3
ETR-B	endothelin receptor B
FBS	fetal bovine serum
FDG	fluorescein di-β-D-galactopyranoside
GFAP	glial fibrillary acidic protein
HNK	Human natural killer
NC	neural crest
P0	myelin protein zero
p75	nerve growth factor receptor p75
Tg	transgenic

References

1 Anderson, D. J. 1997. Cellular and molecular biology of neural crest cell lineage determination. *Trends Genet.* 13:276.
2 Bronner-Fraser, M. 1995. Origin and developmental potential of the neural crest. *Exp. Cell Res.* 218:405.
3 Ito, K. and Sieber-Blum, M. 1993. Pluripotent and developmentally restricted neural-crest-derived cells in posterior visceral arches. *Dev. Biol.* 156:191.
4 Le Douarin, N. M. and Kalcheim, C. 1999. Cell lineage segregation during neural crest ontogeny. In Le Douarin, N. M. and Kalcheim, C., eds., *The Neural Crest*, p. 304. Cambridge University Press, Cambridge.
5 Morrison, S. J., White, P. M., Zock, C. and Anderson, D. J. 1999. Prospective identification, isolation by flow cytometry, and *in vivo* self-renewal of multipotent mammalian neural crest stem cells. *Cell* 96:737.
6 Anderson, G. and Jenkinson, E. J. 2001. Lymphostromal interactions in thymic development and function. *Nat. Rev. Immunol.* 1:30.
7 Bockman, D. E. and Kirby, M. L. 1984. Dependence of thymus development on derivatives of the neural crest. *Science* 223:498.
8 Le Douarin, N. M. and Jotereau, F. V. 1975. Tracing of cells of the avian thymus through embryonic life in interspecific chimeras. *J. Exp. Med.* 142:17.
9 Manley, N. R. and Blackburn, C. C. 2003. A developmental look at thymus organogenesis: where do the non-hematopoietic cells in the thymus come from? *Curr. Opin. Immunol.* 15:225.
10 Merscher, S., Funke, B., Epstein, J. A. *et al.* 2001. TBX1 is responsible for cardiovascular defects in velo-cardio-facial/DiGeorge syndrome. *Cell* 104:619.
11 Epstein, J. A., Li, J., Lang, D. *et al.* 2000. Migration of cardiac neural crest cells in Splotch embryos. *Development* 127:1869.
12 Vitelli, F., Morishima, M., Taddei, I., Lindsay, E. A. and Baldini, A. 2002. Tbx1 mutation causes multiple cardiovascular defects and disrupts neural crest and cranial nerve migratory pathways. *Hum. Mol. Genet.* 11:915.
13 Jiang, X., Rowitch, D. H., Soriano, P., McMahon, A. P. and Sucov, H. M. 2000. Fate of the mammalian cardiac neural crest. *Development* 127:1607.
14 Anderson, G., Moore, N. C., Owen, J. J. and Jenkinson, E. J. 1996. Cellular interactions in thymocyte development. *Annu. Rev. Immunol.* 14:73.
15 Blackburn, C. C. and Manley, N. R. 2004. Developing a new paradigm for thymus organogenesis. *Nat. Rev. Immunol.* 4:278.
16 Kuratani, S. and Bockman, D. E. 1990. Impaired development of the thymic primordium after neural crest ablation. *Anat. Rec.* 228:185.
17 Kuratani, S. and Bockman, D. E. 1990. The participation of neural crest derived mesenchymal cells in development of the epithelial primordium of the thymus. *Arch. Histol. Cytol.* 53:267.
18 Soriano, P. 1999. Generalized lacZ expression with the Rosa26 Cre reporter strain. *Nat. Genet.* 21:70.
19 Yamauchi, Y., Abe, K., Mantani, A. *et al.* 1999. A novel transgenic technique that allows specific marking of the neural crest cell lineage in mice. *Dev. Biol.* 212:191.
20 Yamazaki, H., Yoshino, M. and Hayashi, S. 2005. Neural crest stem cells and organogenesis. In F. Columbus., ed. In *Progress in Stem Cell Research.* Nova Science Publisher Inc. NY, in press.
21 Yamazaki, H., Kurino, T., Sakata, E., Yoshino, M. and Hayashi, S.-I. 2003. Tooth development and tooth regeneration using tooth germ, dental pulp cells, neural crest cells and embryonic stem cells. *Recent Res. Develop. Biophys. Biochem.* 3:907.
22 Baroffio, A., Dupin, E. and Le Douarin, N. M. 1991. Common precursors for neural and mesectodermal derivatives in the cephalic neural crest. *Development* 112:301.
23 Erickson, C. A. and Goins, T. L. 1995. Avian neural crest cells can migrate in the dorsolateral path only if they are specified as melanocytes. *Development* 121:915.
24 Luo, R., Gao, J., Wehrle-Haller, B. and Henion, P. D. 2003. Molecular identification of distinct neurogenic and melanogenic neural crest sublineages. *Development* 130:321.
25 Noden, D. M. 1988. Interactions and fates of avian craniofacial mesenchyme. *Development* 103(Suppl.):121.
26 White, P. M. and Anderson, D. J. 1999. *In vivo* transplantation of mammalian neural crest cells into chick hosts reveals a new autonomic sublineage restriction. *Development* 126:4351.
27 Henion, P. D. and Weston, J. A. 1997. Timing and pattern of cell fate restrictions in the neural crest lineage. *Development* 124:4351.
28 Lahav, R., Dupin, E., Lecoin, L. *et al.* 1998. Endothelin 3 selectively promotes survival and proliferation of neural crest-derived glial and melanocytic precursors *in vitro*. *Proc. Natl Acad. Sci. USA* 95:15214.
29 Baynash, A. G., Hosoda, K., Giaid, A. *et al.* 1994. Interaction of endothelin-3 with endothelin-B receptor is essential for development of epidermal melanocytes and enteric neurons. *Cell* 79:1277.
30 Yoshida, H., Kunisada, T., Kusakabe, M., Nishikawa, S. and Nishikawa, S.-I. 1996. Distinct stages of melanocyte differentiation

revealed by anlaysis of nonuniform pigmentation patterns. *Development* 122:1207.
31 Abe, K., Hashiyama, M., Macgregor, G. and Yamamura, K. 1996. Purification of primordial germ cells from TNAPbeta-geo mouse embryos using FACS-gal. *Dev. Biol.* 180:468.
32 Nishikawa, S., Ogawa, M., Nishikawa, S., Kunisada, T. and Kodama, H. 1988. B lymphopoiesis on stromal cell clone: stromal cell clones acting on different stages of B cell differentiation. *Eur. J. Immunol.* 18:1767.
33 Tsukamoto, K., Jackson, I. J., Urabe, K., Montague, P. M. and Hearing, V. J. 1992. A second tyrosinase-related protein, TRP-2, is a melanogenic enzyme termed DOPAchrome tautomerase. *EMBO J.* 11:519.
34 Yamane, T., Hayashi, S. I., Mizoguchi, M., Yamazaki, H. and Kunisada, T. 1999. Derivation of melanocytes from embryonic stem cells in culture. *Dev. Dyn.* 216:450.
35 Shah, N. M., Marchionni, M. A., Isaacs, I., Stroobant, P. and Anderson, D. J. 1994. Glial growth factor restricts mammalian neural crest stem cells to a glial fate. *Cell* 77:349.
36 Ito, K., Morita, T. and Sieber-Blum, M. 1993. *In vitro* clonal analysis of mouse neural crest development. *Dev. Biol.* 157:517.
37 Yamazaki, H., Kunisada, T., Yamane, T. and Hayashi, S. I. 2001. Presence of osteoclast precursors in colonies cloned in the presence of hematopoietic colony-stimulating factors. *Exp. Hematol.* 29:68.
38 Trentin, A., Glavieux-Pardanaud, C., Le Douarin, N. M. and Dupin, E. 2004. Self-renewal capacity is a widespread property of various types of neural crest precursor cells. *Proc. Natl Acad. Sci. USA* 101:4495.
39 Bronner-Fraser, M. 1986. Analysis of the early stages of trunk neural crest migration in avian embryos using monoclonal antibody HNK-1. *Dev. Biol.* 115: 44.
40 Waldo, K., Lo, C. W. and Kirby, M. L. 1999. Connexin 43 expression reflects neural crest patterns during cardiovascular development. *Dev. Biol.* 208:307.
41 Natoli, T. A., Ellsworth, M. K., Wu, C., Gross, K. W. and Pruitt, S. C. 1997. Positive and negative DNA sequence elements are required to establish the pattern of *Pax3* expression. *Development* 124:617.
42 Pietri, T., Eder, O., Blanche, M., Thiery, J. P. and Dufour, S. 2003. The human tissue plasminogen activator–Cre mouse: a new tool for targeting specifically neural crest cells and their derivatives *in vivo*. *Dev. Biol.* 259:176.
43 Mayer, T. C. 1973. The migratory pathway of neural crest cells into the skin of mouse embryos. *Dev. Biol.* 34:39.
44 Kruger, G. M., Mosher, J. T., Bixby, S., Joseph, N., Iwashita, T. and Morrison, S. J. 2002. Neural crest stem cells persist in the adult gut but undergo changes in self-renewal, neuronal subtype potential, and factor responsiveness. *Neuron* 35:657.
45 Cordier, A. C. and Heremans, J. F. 1975. Nude mouse embryo: ectodermal nature of the primordial thymic defect. *Scand. J. Immunol.* 4:193.
46 Bennett, A. R., Farley, A., Blair, N. F., Gordon, J., Sharp, L. and Blackburn, C. C. 2002. Identification and characterization of thymic epithelial progenitor cells. *Immunity* 16:803.
47 Gill, J., Malin, M., Hollander, G. A. and Boyd, R. 2002. Generation of a complete thymic microenvironment by MTS24(+) thymic epithelial cells. *Nat. Immunol.* 3:635.
48 Manley, N. R. 2000. Thymus organogenesis and molecular mechanisms of thymic epithelial cell differentiation. *Semin. Immunol.* 12:421.
49 Klug, D. B., Carter, C., Gimenez-Conti, I. B. and Richie, E. R. 2002. Cutting edge: thymocyte-independent and thymocyte-dependent phases of epithelial patterning in the fetal thymus. *J. Immunol.* 169:2842.
50 Jenkinson, W. E., Jenkinson, E. J. and Anderson, G. 2003. Differential requirement for mesenchyme in the proliferation and maturation of thymic epithelial progenitors. *J. Exp. Med.* 198:325.
51 Suniara, R. K., Jenkinson, E. J. and Owen, J. J. 2000. An essential role for thymic mesenchyme in early T cell development. *J. Exp. Med.* 191:1051.
52 Suniara, R. K., Jenkinson, E. J. and Owen, J. J. 1999. Studies on the phenotype of migrant thymic stem cells. *Eur. J. Immunol.* 29:75.
53 Wilkinson, B., Owen, J. J. and Jenkinson. E. J. 1999. Factors regulating stem cell recruitment to the fetal thymus. *J. Immunol.* 162:3873.
54 Itoi, M., Kawamoto, H., Katsura, Y. and Amagai, T. 2001. Two distinct steps of immigration of hematopoietic progenitors into the early thymus anlage. *Int. Immunol.* 13:12031.
55 Etchevers, H. C., Vincent, C., Le Douarin, N. M. and Couly, G. F. 2001. The cephalic neural crest provides pericytes and smooth muscle cells to all blood vessels of the face and forebrain. *Development* 128:1059.
56 Bockman, D. E. and Kirby, M. L. 1985. Neural crest interactions in the development of the immune system. *J. Immunol.* 135(Suppl.): 766.
57 Anderson, G., Anderson, K. L., Tchilian, E. Z., Owen, J. J. and Jenkinson, E. J. 1997. Fibroblast dependency during early thymocyte development maps to the CD25+ CD44+ stage and involves interactions with fibroblast matrix molecules. *Eur. J. Immunol.* 27:1200.
58 Salomon, D. R., Mojcik, C. F., Chang, A. C. *et al.* 1994. Constitutive activation of integrin alpha 4 beta 1 defines a unique stage of human thymocyte development. *J. Exp. Med.* 179:1573.
59 Godfrey, D. I., Kennedy, J., Suda, T. and Zlotnik, A. 1993. A developmental pathway involving four phenotypically and functionally distinct subsets of CD3−CD4−CD8− triple-negative adult mouse thymocytes defined by CD44 and CD25 expression. *J. Immunol.* 150:4244.
60 Soriano, P. 1997. The PDGF alpha receptor is required for neural crest cell development and for normal patterning of the somites. *Development* 124:2691.
61 Tallquist, M. D. and Soriano, P. 2003. Cell autonomous requirement for PDGFRalpha in populations of cranial and cardiac neural crest cells. *Development* 130:507.
62 Takakura, N., Yoshida, H., Ogura, Y., Kataoka, H., Nishikawa, S. and Nishikawa, S. 1997. PDGFR alpha expression during mouse embryogenesis: immunolocalization analyzed by whole-mount immunohistostaining using the monoclonal anti-mouse PDGFR alpha antibody APA5. *J. Histochem. Cytochem.* 45:883.
63 Petrie, H. T. 2003. Cell migration and the control of post-natal T-cell lymphopoiesis in the thymus. *Nat. Rev. Immunol.* 3:859.
64 Petrie, H. T. 2002. Role of thymic organ structure and stromal composition in steady-state postnatal T-cell production. *Immunol. Rev.* 189:8.
65 Le Douarin, N. M. 1978. Ontogeny of hematopoietic organs studied in avian embryo interspecific chimeras. In Clarkson, B., Marks, P. A. and Till, J. E., eds., *Differentiation of Normal and Neoplastic Hematopoietic Cells*, p. 5. Cold Spring Harbor Laboratory, Cold Spring Harbor, NY.

ELSEVIER

CYTOKINE

www.elsevier.com/locate/issn/10434666

Cytokine 31 (2005) 288–297

Down-regulation of osteoprotegerin production in bone marrow macrophages by macrophage colony-stimulating factor

Naoko Yamada [a,*], Tohru Tsujimura [a,b], Haruyasu Ueda [b], Shin-Ichi Hayashi [c], Hideki Ohyama [a], Haruki Okamura [b], Nobuyuki Terada [a,b]

[a] *Department of Pathology, Hyogo College of Medicine, Nishinomiya, Hyogo, Japan*
[b] *Laboratory of Host defenses, Institute of Advanced Medical Sciences, Hyogo College of Medicine, Nishinomiya, Hyogo, Japan*
[c] *Department of Immunology, School of Life Science, Faculty of Medicine, Tottori University, Yonago, Tottori, Japan*

Received 14 October 2004; received in revised form 28 January 2005; accepted 14 March 2005

Abstract

Macrophage colony-stimulating factor (M-CSF) and receptor activator of NF-κB ligand (RANKL) induce the differentiation of bone marrow macrophages (BMMs) into osteoclasts. To delineate mechanisms involved, the effect of M-CSF on the production of osteoprotegerin (OPG), decoy receptor of RANKL, in BMMs was investigated. Mouse bone marrow cells were cultured with M-CSF for 4 days and adherent cells formed were used as BMMs. BMMs were cultured with or without M-CSF, and analyzed for expression of OPG and receptor activator of NF-κB (RANK; receptor for RANKL) mRNAs by real-time polymerase chain reaction and secretion of OPG by enzyme-linked immunosorbent assay. BMMs expressed macrophage markers, CD115 (c-fms), Mac-1 and F4/80, and showed phagocytotic activity. In addition, BMMs expressed OPG mRNA and secreted OPG into medium. M-CSF inhibited both the OPG mRNA expression and the OPG secretion dose-dependently and reversibly. The expression of RANK mRNA was not significantly affected by M-CSF. The results showed that M-CSF suppresses the OPG production in BMMs, which may increase the sensitivity of BMMs to RANKL.

Keywords: Macrophage colony-stimulating factor; Osteoprotegerin; Bone marrow macrophage; Osteoclastogenesis

1. Introduction

Osteoclasts, multinucleated cells that resorb bone, are generated from hemopoietic cells of the monocyte/macrophage lineage [1–3]. In this process, bone marrow stromal cells or osteoblasts play a pivotal role through cell-to-cell interaction [3–6]. Stromal cells/osteoblasts express receptor activator of NF-κB ligand (RANKL) on their surface and secrete macrophage colony-stimulating factor (M-CSF). RANKL and M-CSF bind to respective receptors, receptor activator of NF-κB (RANK) and M-CSF receptor (CD115, c-fms), expressed on osteoclast progenitors to induce their differentiation [3,5–12]. Stromal cells/osteoblasts also secrete osteoprotegerin (OPG), a soluble glycoprotein of the tumor necrosis factor receptor superfamily, that acts as a decoy receptor for RANKL competing against RANK and thereby inhibiting osteoclast differentiation [3,8–12]. Various cytokines or hormones exert their effects on osteoclast differentiation by regulating expression of RANKL, M-CSF and OPG in stromal cells or osteoblasts [9,10,12].

Kobayashi et al. [13] have shown that incubation of bone marrow cells with M-CSF in vitro generates adherent cells that express specific macrophage markers

* Corresponding author. Tel.: +81 798 45 6432; fax: +81 798 45 6431.
E-mail address: ynaoko@hyo-med.ac.jp (N. Yamada).

1043-4666/$ - see front matter © 2005 Elsevier Ltd. All rights reserved.
doi:10.1016/j.cyto.2005.03.009

and differentiate into osteoclasts in the presence of M-CSF and RANKL. In this study, we investigated the role of M-CSF in osteoclastogenesis in this system. We found that bone marrow macrophages also produce OPG and that this OPG production was suppressed by M-CSF. These results suggest that M-CSF increases the sensitivity of osteoclast progenitors to RANKL by down-regulation of their OPG production.

2. Results

2.1. Phenotypic analysis of bone marrow macrophages

Mouse bone marrow cells were cultured with recombinant human (rh)M-CSF (100 ng/ml) for 4 days, and adherent cells (bone marrow macrophages; BMMs) were analyzed for expression of various surface antigens by flowcytometry. Essentially all BMMs were positive for specific surface markers for macrophages, Mac-1 (96.9%) and CD115 (M-CSF receptor, c-fms) (95.3%) (Fig. 1B and C). Contour plot analysis showed Mac-1-positive BMMs were homogenous in cell size (Fig. 1A). All BMMs also expressed another macrophage marker, F4/80 (data not shown) while they expressed another macrophage marker, CD14, weakly (Fig. 1D). However, BMMs expressed no specific markers for granulocytes (Gr-1/Ly-6G) (Fig. 1E), NK cells (CD122) (Fig. 1F) and T cells (CD3) (Fig. 1G). Histochemical analysis of 1×10^6 BMMs detected no alkaline phosphatase activity in BMMs. Reverse transcription-polymerase chain reaction (RT-PCR) with total RNA from BMMs showed no expression of calcitonin receptor mRNA (data not shown).

2.2. Phagocytotic activity and osteoclastogenic ability of BMMs

BMMs (Fig. 2A) showed phagocytotic activity (Fig. 2B) but not tartrate-resistant acid phosphatase (TRAP) activity (data not shown). In the presence of rhM-CSF (25 ng/ml), BMMs remained TRAP-negative mononuclear cells after 4 days of culture (Fig. 2C), but in the presence of both rhM-CSF (25 ng/ml) and recombinant human soluble (rhs) RANKL (25 ng/ml), they differentiated into TRAP-positive multinucleated osteoclasts (Fig. 2D). In the presence of rhsRANKL (25 ng/ml), rhM-CSF at 5–50 ng/ml induced osteoclastogenesis of BMMs dose-dependently after 4 and 7 days of culture (Fig. 3A and B).

2.3. Suppression of expression of OPG mRNA and secretion of OPG by M-CSF

Fig. 4A shows the effect of rhM-CSF on OPG mRNA expression in BMMs. Expression of OPG mRNA in BMMs increased with time in culture without rhM-CSF, and was suppressed in the presence of rhM-CSF (25 ng/ml). The amount of OPG secreted in medium was also markedly suppressed by rhM-CSF (25 ng/ml) when expressed as pg OPG/10^4 cells (Fig. 4B-1). The number of viable BMMs after 4 or 7 days of culture was much less in the absence of rhM-CSF than in the presence of rhM-CSF (Fig. 4B-2). However, the concentration of OPG in medium was also decreased by rhM-CSF; average OPG concentrations in medium in culture without rhM-CSF vs. those with rhM-CSF were 236 vs. 111 pg/ml during days 0–4 and 999 vs. 444 pg/ml during days 5–7. The amounts of nitrite plus nitrate in medium on days 0–4 and 5–7 with or without rhM-CSF (25 ng/ml) were below the limit of detection, i.e., 10 μM.

The inhibitory effects of M-CSF on the expression of OPG mRNA was dose-dependent (Fig. 5A), with significant effects on both expression of OPG mRNA and secretion of OPG observed at 10 ng/ml when examined in culture for 4 days (Fig. 5A and B-1). The number of viable BMMs increased dose-dependently (Fig. 5B-2), but the OPG concentration in medium was also decreased in the presence of rhM-CSF. Average OPG concentrations in the medium in the absence of rhM-CSF and in the presence of rhM-CSF at 10, 30 and 60 ng/ml were 120, 49, 52 and 32 pg/ml, respectively. rhsRANKL (25 ng/ml) did not affect OPG mRNA expression in BMMs with or without rhM-CSF (25 ng/ml) (data not shown).

To confirm the production of OPG in BMMs, we performed double-staining analysis of OPG and CD115 (Fig. 6). The results showed that OPG mRNA was expressed in CD115-positive cells.

2.4. Reversible effects of M-CSF on secretion of OPG by BMMs

BMMs were first cultured in the absence of rhM-CSF for 4 days and subsequently in the presence or absence of rhM-CSF (60 ng/ml) for 4 days. The delayed addition of rhM-CSF inhibited the secretion of OPG by BMMs expressed as pg OPG/10^4 cells (Fig. 7A) or a concentration in medium in spite of a difference in viable cell number (Fig. 7B). Average OPG concentrations in the medium in the presence and absence of rhM-CSF were 1992 and 3192 pg/ml, respectively.

We also examined whether the inhibition of OPG secretion by rhM-CSF (60 ng/ml) was reversible by culturing BMMs with rhM-CSF for 4 days, removing rhM-CSF and further culturing for 4 days. The removal of rhM-CSF increased the secretion of OPG by BMMs expressed as pg OPG/10^4 cells (Fig. 7A) or a concentration in medium in spite of a difference in viable cell number (Fig. 7B) although the extent of recovery of OPG secretion was small. Average OPG concentrations

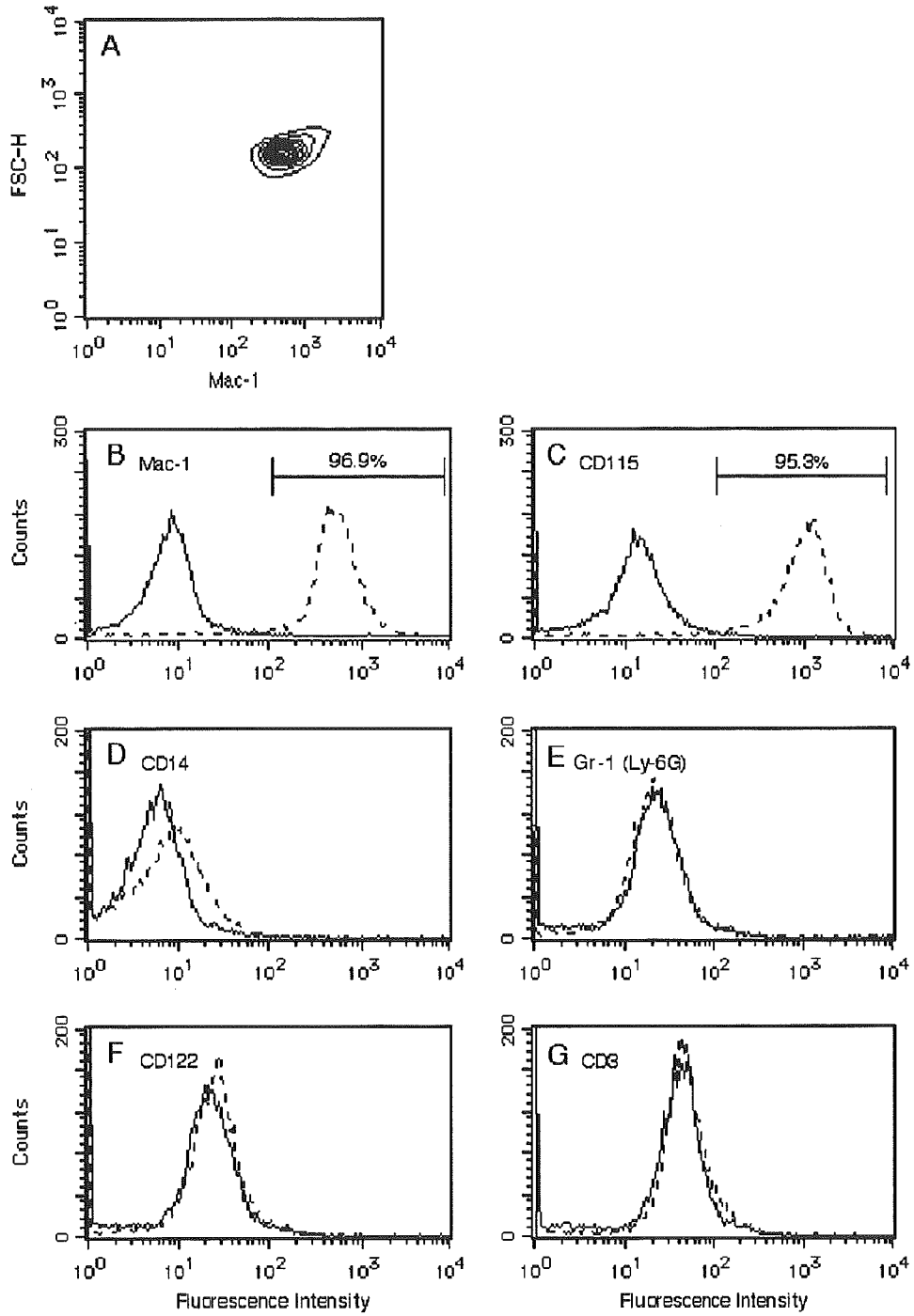

Fig. 1. Phenotypic analysis of BMMs. Bone marrow cells were cultured with rhM-CSF (100 ng/ml) for 4 days, and adherent cells (BMMs) were analyzed for expression of Mac-1 (A, B), CD115 (C), CD14 (D), Gr-1 (E), CD122 (F) and CD3 (G) by flowcytometry. The top figure shows a contour plot analysis for Mac-1 and forward scatters (FSC), and the other figures show histograms for various surface antigens. Dashed and solid lines show profiles with and without antibody, respectively.

in medium in the presence and absence of rhM-CSF were 242 and 653 pg/ml.

2.5. Expression of RANK mRNA in BMMs

Analysis of RANK mRNA showed that BMMs expressed RANK mRNA, and this expression was not significantly affected by M-CSF at concentrations up to 60 ng/ml (Fig. 8).

2.6. Effect of OPG on osteoclastogenesis

To examine the effect of OPG on osteoclastogenesis, BMMs were cultured with rhM-CSF (25 ng/ml),

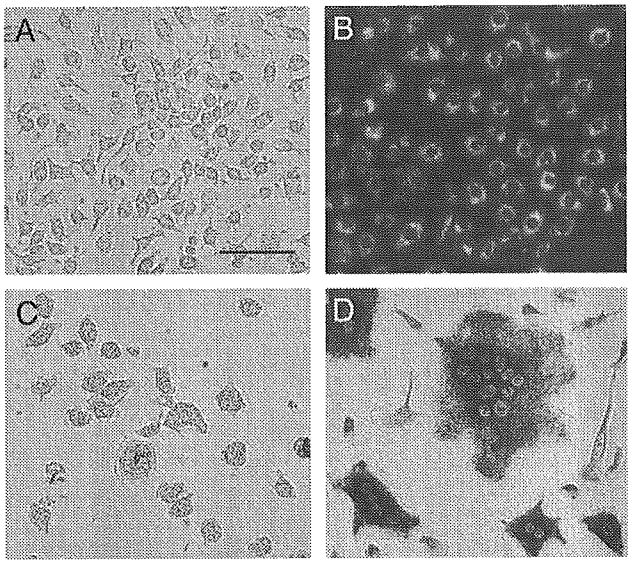

Fig. 2. Phagocytotic and osteoclastogenic activities of BMMs. Bone marrow cells were cultured with rhM-CSF (100 ng/ml) for 4 days, and phagocytotic and osteoclastogenic activities of adherent cells (BMMs) were examined. The phagocytotic activity was assayed by phagocytosis of FITC-labeled beads. The osteoclastogenic activity was estimated by culturing BMMs for 4 days with rhM-CSF (25 ng/ml) and rhsRANKL (25 ng/ml) and by staining for TRAP. (A) BMMs. (B) BMMs showing phagocytosis of FITC-labeled beads. (C) BMMs cultured in the presence of rhM-CSF only, showing no TRAP-positive osteoclasts. (D) BMMs cultured in the presence of rhM-CSF and rhsRANKL, showing TRAP-positive multinucleated osteoclasts. Magnifications of Fig. A–D are same (bar: 50 μm).

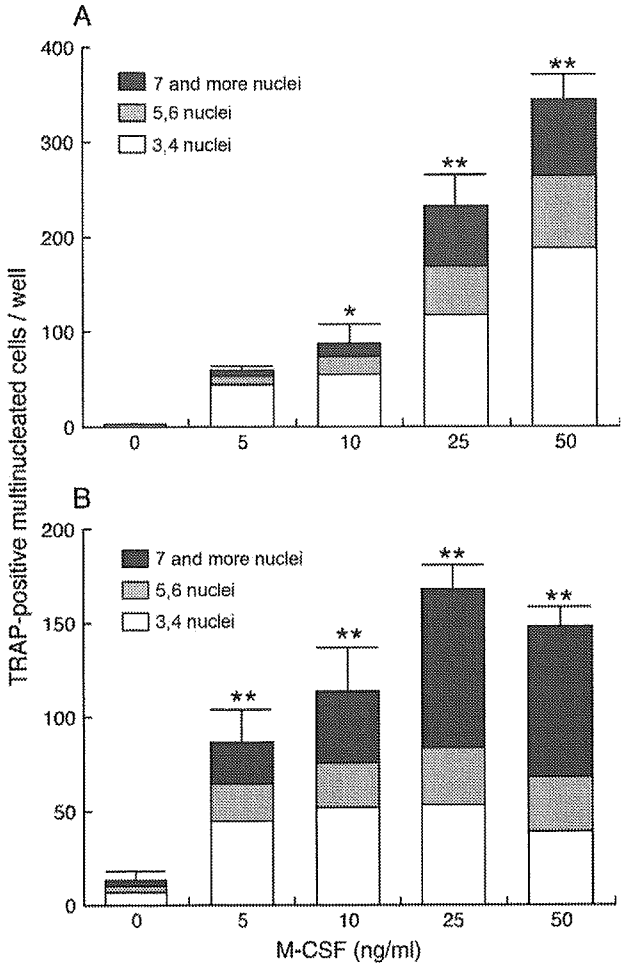

Fig. 3. Dose-dependent effects of M-CSF on the osteoclastogenesis of BMMs. BMMs were cultured with various concentrations of rhM-CSF in the presence of rhsRANKL (25 ng/ml) for 4 days (A) or 7 days (B), and stained for TRAP. TRAP-positive cells with 3 or 4 nuclei, 5 or 6 nuclei or 7 and more nuclei were counted. Each bar represents a mean + SE of total cell numbers for 5 samples. $^{**}P < 0.01$ and $^{*}P < 0.05$, significant difference from values for culture without rhM-CSF (0 ng/ml) by Bonferroni multiple comparison test.

rhsRANKL (25 ng/ml) and 1–100 ng/ml of recombinant mouse (rm) OPG for 4 or 7 days, and analyzed for the formation of multinucleated TRAP-positive osteoclasts. OPG was found to inhibit osteoclastogenesis dose-dependently (Fig. 9).

3. Discussion

Essentially all BMMs used in this study were positive for macrophage surface markers, Mac-1 (96.9%), CD115 (M-CSF receptor, c-fms) (95.3%) and F4/80 (100%), and showed phagocytotic activity, indicating that they were macrophages. Treatment of these cells with M-CSF and sRANKL induced TRAP activity with the formation of multinucleated osteoclasts. These results indicated that BMMs used were likely to have been osteoclast progenitors, as reported by Kobayashi et al. [13].

BMMs used in this study were adherent cells formed when bone marrow cells were incubated with M-CSF for 4 days. Among bone marrow cells, stromal cells, osteoblasts and osteoclasts have been shown to produce OPG [9,14]. Stromal cells and osteoblasts express alkaline phosphatase [15], and osteoclasts TRAP. However, BMMs used in this study were negative for both alkaline phosphatase and TRAP, showing no contamination of stromal cells, osteoblasts and osteoclasts. On the other hand, BMMs were positive for both CD115, macrophage marker, and OPG, indicating that BMMs themselves produce OPG. OPG mRNA is expressed in various tissues such as lung, heart, kidney, liver, thyroid, spinal cord, brain and placenta, in addition to bone marrow stromal cells, osteoblasts and osteoclasts [9,14,16]. Moreover, endothelial cells, aorta smooth muscle cells, fibroblasts, T and B lymphocytes, dendritic cells and various tumor cell lines have been reported to express OPG mRNA [9,12,14]. The present results show that BMMs are an additional potential source of OPG.

The removal of M-CSF increased the secretion of OPG by BMMs but the extent of recovery of the OPG secretion was small. This may be partly due to the

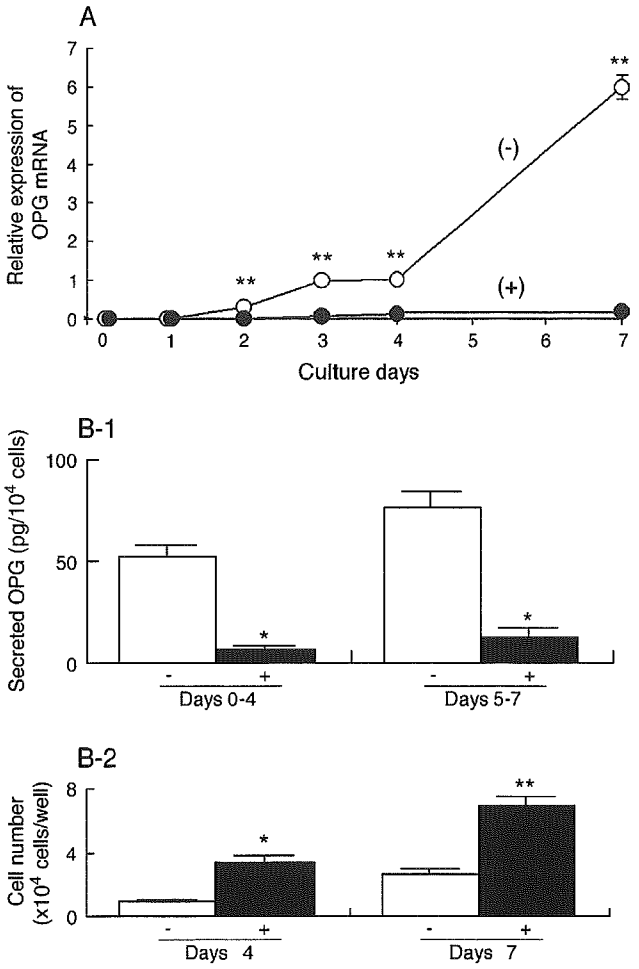

Fig. 4. Time-course analysis of effects of M-CSF on the expression of OPG mRNA and the secretion of OPG by BMMs. BMMs were cultured with (+) or without (−) rhM-CSF (25 ng/ml) for 7 days. (A) OPG and GAPDH mRNAs were estimated on different days by real-time PCR. OPG mRNA values were normalized to GAPDH mRNA values and expressed relative to OPG mRNA expressed in control cells without M-CSF on day 4. Each point represents a mean ± SE for 5 samples. $^{**}P < 0.01$, significant difference from values for culture with rhM-CSF on the same day by Student's *t*-test. (B) OPG secreted into medium during days 0–4 or days 5–7 (B-1) and viable cell number on days 4 and 7 (B-2). Each point represents a mean + SE for 5 samples. $^{**}P < 0.01$ and $^{*}P < 0.05$, significant difference from values for culture without rhM-CSF by Student's *t*-test.

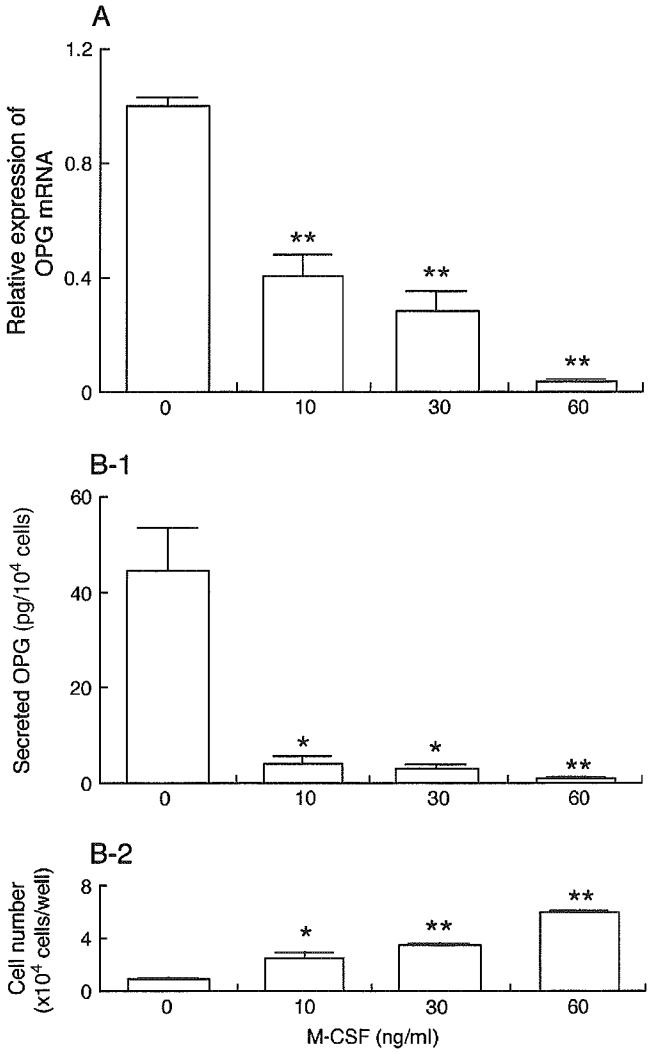

Fig. 5. Dose-dependent inhibition of expression of OPG mRNA and secretion of OPG by M-CSF. BMMs were cultured with various concentrations of rhM-CSF for 4 days, and analyzed for OPG mRNA and secreted OPG. (A) Effect of M-CSF on OPG mRNA expression. OPG mRNA expression was normalized to GAPDH mRNA expression and expressed relative to OPG mRNA expressed in control cells without M-CSF. (B) Effect of M-CSF on OPG secretion (B-1) and viable cell number (B-2). Each bar represents a mean + SE for 5 samples. $^{**}P < 0.01$ and $^{*}P < 0.05$, significant difference from values for culture without M-CSF by Bonferroni multiple comparison test.

sustaining intracellular effects of M-CSF after deprivation of M-CSF in terms of OPG production.

In the in vitro system of osteoclastogenesis using BMMs, 25 ng/ml of rhM-CSF seem to be its adequate but not pharmacological concentration for induction of osteoclastogenesis in the presence of rhsRANKL (25 ng/ml) (Fig. 3) and rhM-CSF at this concentration suppressed the OPG production in BMMs markedly. OPG is a decoy receptor which blocks binding of RANKL to RANK [8–12]. Consistently, we observed that OPG at 1 ng/ml inhibited osteoclastogenesis of BMMs induced by rhM-CSF (25 ng/ml) and rhsRANKL (25 ng/ml). Furthermore, we observed that in the absence of M-CSF, the average concentration of OPG in medium after 7 days of culture was more than 1 ng/ml (Fig. 4; average OPG concentrations during days 0–4 and days 5–7 were 236 and 998 pg/ml, respectively) suggesting that without M-CSF, BMMs secrete a relatively large amount of OPG which may interfere with the action of RANKL, thus suppressing osteoclastogenesis. Therefore, the suppression by M-CSF of the OPG production in osteoclast progenitors seems to play a role in increasing the sensitivity of osteoclast progenitors to RANKL at least in this in vitro system of osteoclastogenesis.

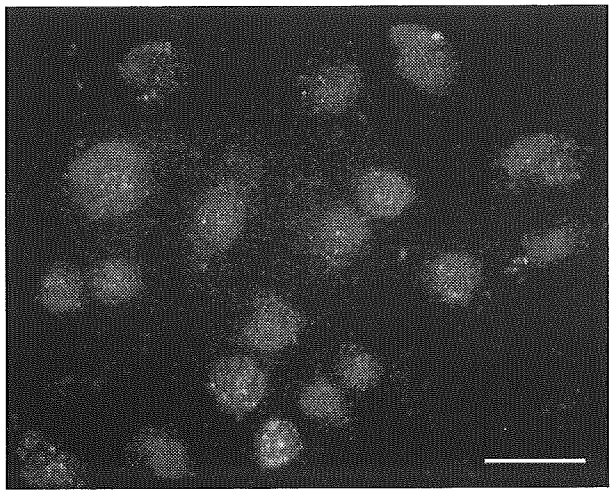

Fig. 6. Analysis of CD115 and OPG in BMMs by double staining. BMMs were cultured without rhM-CSF (25 ng/ml) for 7 days, and stained with FITC-labeled anti-CD115 (green) and rhodamin-labeled anti-OPG (red) antibodies. Bar: 20 μm.

In osteoclastogenesis mediated by bone marrow stromal cells or osteoblasts, several hormones and cytokines, such as parathyroid hormone, glucocorticoid, vitamin D_3, prostaglandin E_2, IL-1, TNF-α, IL-11, have been shown to stimulate osteoclastogenesis by increasing

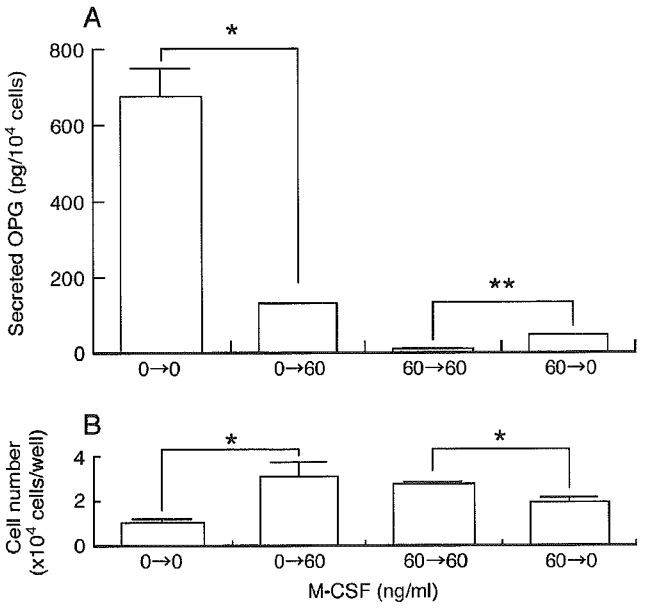

Fig. 7. Effects of the delayed addition and removal of M-CSF on OPG secretion. In one experiment, BMMs were first cultured without rhM-CSF for 4 days, then with (0 → 60) or without (0 → 0) rhM-CSF (60 ng/ml) for further 4 days and analyzed for OPG in medium. In another experiment, BMMs were first cultured with rhM-CSF (60 ng/ml) for 4 days, then with (60 → 60) or without (60 → 0) rhM-CSF (60 ng/ml) for further 4 days, and analyzed for OPG in medium. (A) Secreted OPG in medium during the second culture. (B) Number of viable cells at the end of culture. Each bar represents a mean + SE for 5 samples. $^{**}P < 0.01$ and $^{*}P < 0.05$, significant difference by Student's *t*-test.

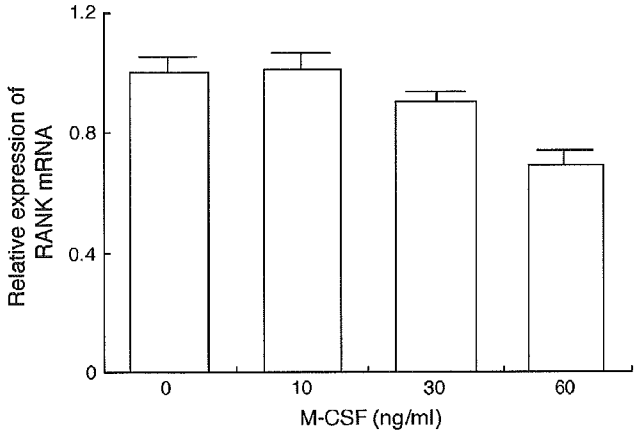

Fig. 8. Effect of M-CSF on expression of RANK mRNA. BMMs were cultured with various concentrations of rhM-CSF for 4 days, and analyzed for RANK and GAPDH mRNAs by real-time PCR. RANK mRNA expression was normalized to GAPDH mRNA expression and expressed relative to RANK mRNA expressed in control cells without M-CSF. Each bar represents a mean + SE for 5 samples. There were no significant differences among values at various concentrations of rhM-CSF by Bonferroni multiple comparison test.

relative expression of RANKL to OPG in stromal cells or osteoblasts [9,10,12]. The present in vitro study showed that osteoclast progenitors themselves produce OPG, and that M-CSF, the other obligatory requirement for osteoclastogenesis besides RANKL, suppresses their OPG production in favor of osteoclastogenesis. However, some cytokines, such as TNF-α, IL-6 and IL-11, exert effects directly on osteoclast progenitors to induce osteoclastogenesis in the presence of M-CSF by a RANKL-independent mechanism [13,17–19]. Therefore, the inhibitory effect of M-CSF on the OPG production by osteoclast progenitors does not appear to be essential for RANKL-independent osteoclastogenesis although it is important for RANKL-dependent osteoclastogenesis.

Wang et al. [20] have reported that the OPG production by bone marrow stromal cells is increased by nitric oxide. Therefore, the involvement of nitric oxide in the inhibitory effect of M-CSF on the OPG production by BMMs was examined. However, the amount of metabolites of nitric oxide, nitrite plus nitrate, in medium was too small to assess a role of nitric oxide in the OPG production by BMMs. Further studies with nitric oxide donor or using an inducible nitric oxide synthase (NOS) knockout mouse are desired.

M-CSF exerted no significant effect on RANK mRNA expression in BMMs. Arai et al. [21] reported that M-CSF induced RANK expression in c-kit-positive, c-fms-positive and Mac-1-negative bone marrow mononuclear osteoclast progenitors which did not express RANK. Cappellen et al. [22] also reported that M-CSF up-regulated expression of RANK mRNA in bone marrow mononuclear osteoclast progenitors which expressed little mRNAs of c-fms and RANK. Bone

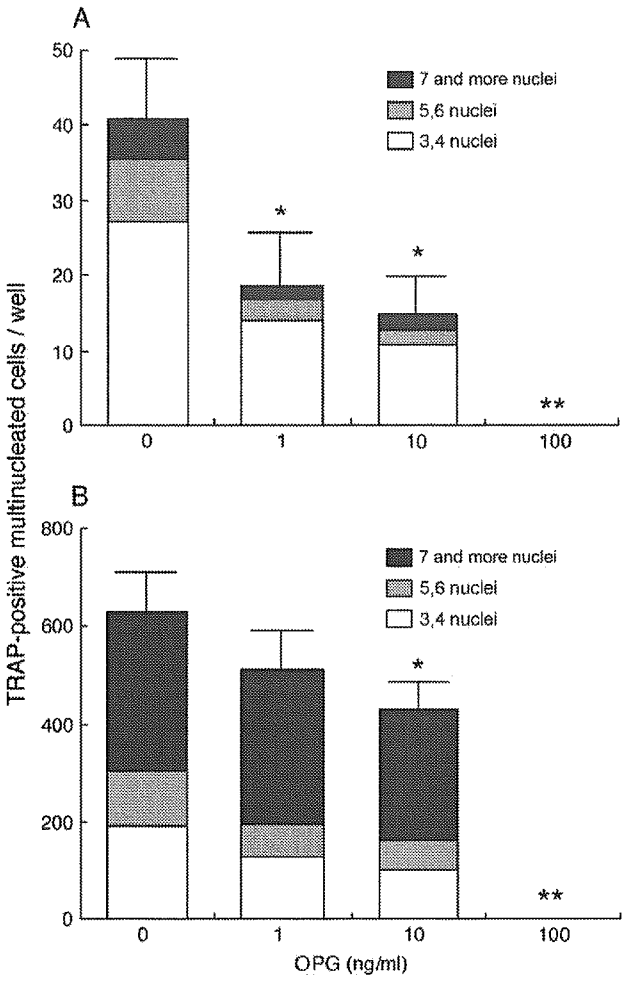

Fig. 9. Effect of OPG on osteoclastogenesis of BMMs. BMMs were cultured with rhM-CSF (25 ng/ml) and rhsRANKL (25 ng/ml) in the presence of various concentrations of rmOPG for 4 days (A) or 7 days (B), and stained for TRAP. TRAP-positive cells with 3 or 4 nuclei, 5 or 6 nuclei or 7 and more nuclei were counted. Each bar represents a mean + SE of total cell numbers for 5 samples. $^{**}P < 0.01$ and $^{*}P < 0.05$, significant difference from values for culture without OPG (0 ng/ml) by Bonferroni multiple comparison test.

marrow mononuclear osteoclast progenitors used in the studies of Arai et al. [21] and Cappellen et al. [22] were not treated with M-CSF during preparation of osteoclast progenitors. However, BMMs used in this study had been exposed to rhM-CSF (100 ng/ml) for 4 days, and were Mac-1-, c-fms- and CD14-positive and expressed RANK mRNA. As shown by Takeshita et al. [23] and Cappellen et al. [22], M-CSF plays roles of a differentiation factor as well as a growth factor for osteoclast early progenitors. Therefore, the difference in the effect of M-CSF on RANK expression between studies of Arai et al. [21] and Cappellen et al. [22], and ours seems to be derived from different stages of differentiation of osteoclast progenitors used in the study.

In conclusion, the present study shows that M-CSF suppresses the production of OPG in BMMs in vitro, which, if occurs in vivo, indicates that M-CSF may act to increase the sensitivity of osteoclast progenitors to RANKL.

4. Materials and methods

4.1. Materials

Recombinant human soluble (rhs) RANKL was purchased from PeproTech (London, UK), and recombinant mouse (rm) OPG from R & D Systems (Minneapolis, MN). Biotinylated rat anti-mouse CD115 (c-fms) antibody, FITC-labeled rat anti-mouse Mac-1 antibody, Cychrome-labeled rat anti-mouse CD3 antibody, PE-labeled rat anti-mouse CD14, PE-labeled rat anti-mouse CD122 and Gr-1 (Ly-6G) antibodies, Cychrome-conjugated streptavidin, FITC-conjugated avidin and Fc-block were purchased from BD Biosciences (San Jose, CA), rabbit anti-mouse OPG antibody and rhodamin-conjugated anti-rabbit IgG from Santa Cruz Biotechnology (Santa Cruz, CA), rat anti-mouse F4/80 antibody from Biomedicals AG (Rheinstrasse, Augst, Switzerland), Fluospheres (FITC-labeled microspheres) from Invitrogen (Carlsbad, CA), and Fast Blue Salt BB and naphthol AS-BI phosphoric acid from Sigma (St. Louis, MO). A mouse OPG enzyme-linked immunosorbent assay (ELISA) kit was purchased from Techne (Minneapolis, MN), a nitrite/nitrate assay kit from Wako (Osaka, Japan), and a leukocyte acid phosphatase kit from Sigma. Recombinant human (rh)M-CSF was kindly provided by Dr. T. Kuhara (Morinaga Milk Industry; Tokyo, Japan).

4.2. Mice

Male Balb/c mice of 7 weeks of age were purchased form Japan SLC (Hamamatsu, Shizuoka, Japan). Mice were kept at 25 °C under controlled light conditions (12 h light/12 h dark), and allowed free access to water and a pellet diet. All experiments conformed to the guidelines for the "Care and Use of Animals" in the Information for Authors Section of the American Journal of Physiology, and were approved by the Animal Care Committee of Hyogo College of Medicine.

4.3. Isolation of bone marrow macrophages

The femurs and tibias of 7-week-old mice were aseptically removed and dissected free of adhering tissues. The bone ends were cut off with scissors and the marrow cavity was flushed with α-Minimal Essential Medium (α-MEM) by slowly injecting at one end of the bone using a sterile needle to collect bone marrow cells. These cells were washed with α-MEM, and red blood cells contained were burst by treatment with 155 mM

NH_4Cl, pH 7.3, containing 14.2 mM $NaHCO_3$ and 1 mM ethylenediaminetetraacetic acid disodium salt (EDTA). Cells were washed with Ca^{++}, Mg^{++}-free Dulbecco's phosphate-buffered saline, pH 7.4 (PBS), and cultured at 5×10^6 cells/10 cm tissue culture dish in 10 ml of α-MEM containing 10% fetal bovine serum (FBS), 100 IU/ml penicillin G and 100 μg/ml streptomycin with rhM-CSF (100 ng/ml). Floating cells were removed and attached cells were harvested by treatment with PBS containing 0.02% EDTA and used as bone marrow macrophages (BMMs).

4.4. Flowcytometry

BMMs were suspended in ice-cold PBS containing 2% FBS (PBS–FBS). Cells were incubated in Fc-block diluted with PBS (1:25 dilution) on ice for 30 min and subsequently with FITC-labeled Mac-1, Cychrome-labeled CD3, PE-labeled Gr-1, PE-labeled CD14, PE-labeled CD122 or biotinylated CD115 antibody (1:100 dilution for each antibody) on ice for 30 min. When cells were incubated with biotinylated CD115 antibody, cells were washed with PBS–FBS and further incubated with Cychrome-conjugated streptavidin (1:200 dilution) on ice for 30 min. Cells were then washed with PBS–FBS and analyzed by an FACS Calibur flowcytometer (Becton Dickinson; Mountain View, CA).

4.5. Alkaline phosphatase staining

BMMs obtained as described above were collected on glass slides using a Shandon Cytospin 3 cytocentrifuge (Thermo Electron Corp.; Wltham, MA) and fixed in 3.7% formaldehyde in methanol for 30 s at 4 °C. The cells were then incubated with a freshly prepared alkaline phosphatase substrate solution (0.2 M Tris–HCl buffer, pH 9.2, containing 1 mg/ml Fast Blue Salt BB and 1 mg/ml naphthol AS-BI phosphoric acid) for 60 min at room temperature. The reaction was terminated by removal of the substrate solution and washing with water. After counterstaining with hematoxylin, 1×10^6 cells were examined for the expression of alkaline phosphatase activity.

4.6. Reverse transcription-polymerase chain reaction (RT-PCR)

Total RNA was extracted from BMMs in dishes using TRIZOL reagent (Invitrogen; Carlsbad, CA). First strand cDNA was synthesized from 1 μg of total RNA with a random primer and Superscript II Reverse Transcriptase (Invitrogen), and an aliquot of the cDNA was subjected to PCR amplification with EX *Taq* polymerase (Takara; Tokyo, Japan) using the following specific PCR primers: a sense primer, 5′-AAGCACAT GTTCCTTACTTA-3′ (1060–1079) and an antisense primer, 5′-ACAAACTGGATCCCCAGCAGGGGCA C-3′ (1663–1688) for the mouse *calcitonin receptor* gene and a sense primer, 5′-GGGTTCCCATAAAGTCACT CTG-3′ (266–287) and an antisense primer, 5′-TCAG TCTATGTCCTGAACTTTGAA-3′ (633–654) for the mouse *β-actin* gene. The PCR conditions were 94 °C for 30 s, 58 °C for 30 s, and 72 °C for 1 min for 35 cycles, with a gene-Amp PCR system 2400 (Perkin–Elmer; Norwalk, CT). The amplified fragments were detected in the expected sizes by ethidium bromide staining in a 1% agarose gel.

4.7. Phagocytotic activity of BMMs

Bone marrow cells obtained as described above were cultured in 96-well plate at 1×10^5 cells/well in 0.2 ml of α-MEM containing 10% FBS with rhM-CSF (100 ng/ml) for 4 days, and adherent cells (BMMs) formed were cultured in α-MEM containing 10% FBS with Fluospheres (1:1000 dilution) for 3 h. After washing with PBS, cells were examined with a fluorescence microscope (Nikon; Tokyo, Japan) and picture analyzer software (AQUACOSMOS) (Hamamatsu Photonics; Hamamatsu, Shizuoka, Japan).

4.8. Tartrate-resistant acid phosphatase (TRAP) staining

BMMs seeded in 96-well plates (1×10^5 cells/well) were cultured in 0.2 ml per well of α-MEM containing 10% FBS with rhM-CSF (25 ng/ml) only, with rhM-CSF (5, 10, 25 or 50 ng/ml) and rhsRANKL (25 ng/ml) or with rhM-CSF (25 ng/ml), rhsRANKL (25 ng/ml) and various concentrations of rmOPG for 4 or 7 days. After culture, cells were fixed and stained for TRAP using a leukocyte acid phosphatase kit. TRAP-positive multinucleated cells were counted as multinucleated osteoclasts.

4.9. Real-time PCR

BMMs were seeded in a 60-mm tissue culture dish (2.5×10^6 cells/dish) and cultured in 5 ml of α-MEM containing 10% FBS with rhM-CSF at various concentrations. Medium was changed after 4 days. Total RNA was extracted using TRIZOL reagent (Invitrogen). First strand cDNA was synthesized from 1 μg of total RNA with a random primer and Superscript II Reverse Transcriptase (Invitrogen). Real-time PCR analysis of mouse OPG, RANK or GAPDH was performed using the real-time PCR kits with an ABI PRISM 7900HT (Applied Biosystems; Foster, CA). The PCR condition was denaturation at 95 °C for 15 s, and annealing and extension at 60 °C for 1 min, for 40 cycles.

4.10. OPG assay

BMMs were seeded in 96-well plates (1×10^5 cells/well) and cultured in 0.2 ml per well of α-MEM containing 10% FBS with rhM-CSF at an indicated concentration for 4, 7 or 8 days. Medium was changed after 4 days. After culture, attached cells were harvested by treatment with PBS containing 0.02% EDTA and viable cells were counted by the trypan blue exclusion test. OPG in medium was determined using a mouse OPG ELISA kit. The sensitivity of the assay was 10 pg/ml, and the intra- and inter-assay coefficients of variation were within 6% and 11%, respectively. The amount of OPG secreted in medium was expressed as pg/10^4 cells.

4.11. Assay of nitrite and nitrate

BMMs were seeded in 96-well plates (1×10^5 cells/well) and cultured in 0.2 ml per well of α-MEM without phenol red (Invitrogen) containing 10% FBS with rhM-CSF (25 ng/ml) for 7 days. The amounts of nitrite plus nitrate in medium on days 0–4 and 5–7 were assayed using a nitrite/nitrate assay kit. The lower limit of an assay of this kit was 10 μM.

4.12. Double-staining of CD115 and OPG

BMMs seeded on Lab-Tec chamber slides (Nalge Nunc Int.; Chester, NY) were cultured in α-MEM containing 10% FBS without rhM-CSF for 7 days, fixed in 4% paraformaldehyde for 1 h and treated in PBS containing 0.2% Triton X100 for 15 min. After incubation with PBS containing 2% bovine serum albumin (BSA) for 30 min at room temperature, BMMs were incubated with biotin-conjugated anti-mouse CD115 antibody (1:100 dilution) and rabbit anti-mouse OPG antibody (1:100 dilution) at 37 °C for 1 h, and subsequently with FITC-conjugated avidin (1:100 dilution) and rhodamin-conjugated anti-rabbit IgG (1:100 dilution) at 37 °C for 30 min. BMMs on slides were mounted in 50% glycerin and examined with a fluorescence microscope (Nikon) and picture analyzer software (ARGUS) (Hamamatsu Photonics).

4.13. Statistical analysis

Data are presented as means ± SE. Data of 3 groups or more were analyzed with Bonferroni multiple comparison test and data of 2 groups were analyzed with Student's *t*-test. A P value less than 0.05 was considered significant.

Acknowledgments

This work was supported in part by a Grant-in-Aid for Researchers, Hyogo College of Medicine, and a Hitec Research Center grant and a Grant for Scientific Research from the Japanese Ministry of Education, Culture, Sports, Science and Technology.

The authors thank Dr. H. Tsutsui, Dr. Y. Yasuda and Ms. H. Takeda for their technical support.

References

[1] Udagawa N, Takahashi N, Akatsu T, Tanaka H, Sasaki T, Nishihara T, et al. Origin of osteoclasts: mature monocytes and macrophages are capable of differentiating into osteoclasts under a suitable microenvironment prepared by bone marrow-derived stromal cells. Proc Natl Acad Sci U S A 1990;87:7260–4.

[2] Hayashi S, Yamane T, Miyamoto A, Hemmi H, Tagaya H, Tanio Y, et al. Commitment and differentiation of stem cells to the osteoclast lineage. Biochem Cell Biol 1998;76:911–22.

[3] Suda T, Takahashi N, Udagawa N, Jimi E, Gillespie MT, Martin TJ. Modulation of osteoclast differentiation and function by the new members of the tumor necrosis factor receptor and ligand families. Endocr Rev 1999;20:345–57.

[4] Jimi E, Nakamura I, Amano H, Taguchi Y, Tsurukai T, Tamura M, et al. Osteoclast function is activated by osteoblastic cells through a mechanism involving cell-to-cell contact. Endocrinology 1996;137:2187–90.

[5] Takahashi N, Udagawa N, Suda T. A new member of tumor necrosis factor ligand family, ODF/OPGL/TRANCE/RANKL, regulates osteoclast differentiation and function. Biochem Biophys Res Commun 1999;256:449–55.

[6] Yasuda H, Shima N, Nakagawa N, Yamaguchi K, Kinosaki M, Goto M, et al. A novel molecular mechanism modulating osteoclast differentiation and function. Bone 1999;25:109–13.

[7] Yasuda H, Shima N, Nakagawa N, Yamaguchi K, Kinosaki M, Mochizuki S, et al. Osteoclast differentiation factor is a ligand for osteoprotegerin/osteoclastogenesis-inhibitory factor and is identical to TRANCE/RANKL. Proc Natl Acad Sci U S A 1998;95:3597–602.

[8] Chambers TJ. Regulation of the differentiation and function of osteoclasts. J Pathol 2000;192:4–13.

[9] Hofbauer LC, Khosla S, Dunstan CR, Lacey DL, Boyle WJ, Riggs BL. The roles of osteoprotegerin and osteoprotegerin ligand in the paracrine regulation of bone resorption. J Bone Miner Res 2000;15:2–12.

[10] Boyle WJ, Simonet WS, Lacey DL. Osteoclast differentiation and activation. Nature 2003;423:337–42.

[11] Teitelbaum SL, Ross FP. Genetic regulation of osteoclast development and function. Nat Rev Genet 2003;4:638–49.

[12] Schoppet M, Preissner KT, Hofbauer LC. RANK ligand and osteoprotegerin: paracrine regulators of bone metabolism and vascular function. Arterioscler Thromb Vasc Biol 2002;22:549–53.

[13] Kobayashi K, Takahashi N, Jimi E, Udagawa N, Takami M, Kotake S, et al. Tumor necrosis factor alpha stimulates osteoclast differentiation by a mechanism independent of the ODF/RANKL–RANK interaction. J Exp Med 2000;191:275–86.

[14] Woo KM, Choi Y, Ko SH, Ko JS, Oh KO, Kim KK. Osteoprotegerin is present on the membrane of osteoclasts isolated from mouse long bones. Exp Mol Med 2002;34:347–52.

[15] Takahashi N, Akatsu T, Udagawa N, Sasaki T, Yamaguchi A, Moseley JM, et al. Osteoblastic cells are involved in osteoclast formation. Endocrinology 1988;123:2600–2.

[16] Simonet WS, Lacey DL, Dunstan CR, Kelley M, Chang MS, Luthy R, et al. Osteoprotegerin: a novel secreted protein involved in the regulation of bone density. Cell 1997;89:309–19.
[17] Azuma Y, Kaji K, Katogi R, Takeshita S, Kudo A. Tumor necrosis factor-alpha induces differentiation of and bone resorption by osteoclasts. J Biol Chem 2000;275:4858–64.
[18] Kudo O, Fujikawa Y, Itonaga I, Sabokbar A, Torisu T, Athanasou NA. Pro-inflammatory cytokine (TNF-α/IL-1α)-induction of human osteoclast formation. J Pathol 2002;198:220–7.
[19] Kudo O, Sabokbar A, Pocock A, Itonaga I, Fujiwara Y, Athanasou NA. Interleukin-6 and interleukin-11 support human osteoclast formation by a RANKL-independent mechanism. Bone 2003;32:1–7.
[20] Wang FS, Wang CJ, Chen YJ, Huang YT, Huang HC, Chang PR, et al. Nitric oxide donor increases osteoprotegerin production and osteoclastogenesis inhibitory activity in bone marrow stromal cells from ovariectomized rats. Endocrinology 2004;145:2148–56.
[21] Arai F, Miyamoto T, Ohneda O, Inada T, Sudo T, Brasel K, et al. Commitment and differentiation of osteoclast precursor cells by the sequential expression of c-Fms and receptor activator of nuclear factor κB (RANK) receptors. J Exp Med 1999;190:1741–54.
[22] Cappellen D, Luong-Nguyen NH, Bongiovanni S, Grenet O, Wanke C, Susa M. Transcriptional program of mouse osteoclast differentiation governed by the macrophage colony-stimulating factor and the ligand for the receptor activator of NFκB. J Biol Chem 2002;277:21971–82.
[23] Takeshita S, Arai S, Kudo A. Identification and characterization of mouse bone marrow stromal cell lines immortalized by temperature-sensitive SV40 T antigen: supportive activity for osteoclast differentiation. Bone 2001;29:236–41.